Structure of POPC lipid bilayers in OPLS3e force field

Milla Lindström[1], Antti Poso[1], Piia Bartos[1]‡, Markus S. Miettinen[2]‡*

‡These authors contributed equally.

[1]University of Eastern Finland, School of Pharmacy, Kuopio Campus, Yliopistonranta 1 C, P.O. BOX 1627, 70211 Kuopio

[2]Department of Chemistry, University of Bergen, Bergen, Norway

Computational Biology Unit, Department of Informatics, University of Bergen, Bergen, Norway

*to whom correspondence should be addressed.

*Email: piia.bartos@uef.fi

It is crucial for molecular dynamics simulations of biomembranes that the force field parameters give a realistic model of the membrane behavior. In this study, we examined the OPLS3e force field for the carbon–hydrogen order parameters S_{CH} of POPC (1-palmitoyl-2-oleylphosphatidylcholine) lipid bilayers at varying hydration conditions and ion concentrations. The results show that OPLS3e behaves similarly to the CHARMM36 force field and relatively accurately follows the experimentally measured S_{CH} for the lipid headgroup, the glycerol backbone, and the acyl tails. Thus, OPLS3e is a good choice for simulations of most membrane systems. The exception are systems with an abundancy of ions, as similarly to most other force fields OPLS3e strongly overestimates the membrane-binding of cations, especially Ca^{2+}. This leads to undesirable positive charge of the membrane surface and drastically lowers the concentration of Ca^{2+} in the

surrounding solvent, which might cause issues in systems sensitive to correct charge distribution profiles across the membrane.

INTRODUCTION

Membranes function as biological barriers that separate cells from the environment and delineate different cellular compartments; they are crucial in maintaining the life sustaining chemical and electrical gradients. The key structural constituents of membranes are phospholipids that form the membrane surface with their polar head groups and the membrane core with their lipophilic tails (Fig 1). In addition to phospholipids, biological membranes contain for example cholesterol, proteins, ions, and oligosaccharides. Lipid bilayers play central role in several biological and pathological processes such as cell division, intracellular membrane trafficking, and formation of lipid rafts (1, 2). To fully understand these processes, atomistic and molecular level understanding of lipids is required (3). Such understanding can be obtained through computational tools, but it is important that tools used depict the structure, dynamics, and function of lipid bilayers accurately. Accurate lipid models allow the reliable study of, for example, membrane-bound proteins, transport through membranes, and pharmacokinetics of drugs (4).

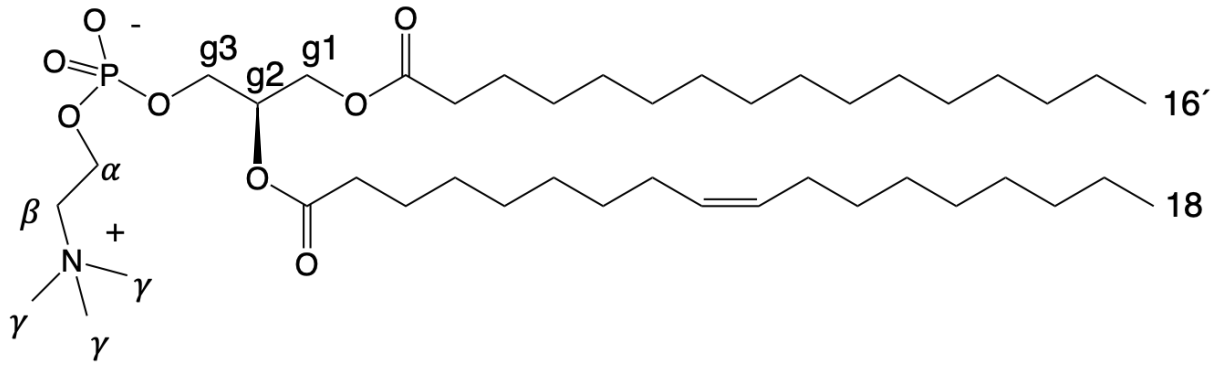

Figure 1. Chemical structure of 1-palmitoyl-2-oleylphosphatidylcholine (POPC)

Why accurate force field parameters are important

Force field accuracy is of key importance in atomistic molecular dynamics (MD) simulation methods. Atomistic MD enables studying systems of interest in life sciences by a balance between computing power and precision: instead of the computationally heavy methods needed to describe quantum mechanical behavior, MD uses typically classical mechanics approximation (called force field) to reproduce molecular behavior. Thus, the validity of MD simulation studies relies heavily on the accuracy of the force field. Not surprisingly, a lot of effort has been gone into force field development since start of MD simulation studies in the 1980s (5, 6).

OPLS3e forcefield

OPLS3e is one of the most recent updates in the OPLS force field series available in the Schrödinger software suite (7). OPLS3e has become widely used in drug discovery and material sciences due to its wide coverage of small molecules and accurate description of protein–ligand interactions. OPLS3e relies heavily on the earlier OPLS3 force field (8), but with addition and refinement of torsional parameters and better handling of partial charges to offer improved accuracy on small–molecule conformational propensities, solvation, and protein-ligand binding. OPLS3e supports membrane simulations and offers optimized parameters for certain lipids: POPC, DMPC (1-2-dimyristoylphosphatidylcholine), DPPC (1-2-dipalmitoylphosphatidylcholine), and POPE (1-palmitoyl-2-oleoyl-phosphoethanolamine). However, to our knowledge the accuracy of lipid simulations in OPLS3e, or its predecessor OPLS3, have not been reported. To examine the performance of OPLS3e and get an insight into how realistic model of lipid bilayers it produces, we simulated pure POPC bilayers at different conditions using the OPLS3e force field. We chose POPC among the OPLS3e-parametrized lipids because of its abundance in biological membranes and the availability of experimental data in the literature.

Performance of a force field can be assessed by comparing different observables between relevant experiments and MD simulations. For membrane lipids, the C–H bond order parameters S_{CH} offer an appealing option for such a task since they can be accurately measured experimentally using ^{2}H-NMR (9) or ^{1}H-^{13}C NMR (10-12) techniques, and easily and directly be calculated in MD simulations. The S_{CH} have a long history in force field validation for lipids and a large amount of experimental data is available in the literature (3). Finally, as S_{CH} can be calculated for every C–H bond of the lipid molecule, they offer a very localized picture of the possible deficiencies of the simulation model (3).

Lipids in other force fields

Previous studies comparing experimental data to simulations show that in general, acyl chains of lipids are usually quite well described in simulations, and agreement of the structure and behavior of this region between the simulation and the experimental data is quite good (3, 13-15). However, correct description of headgroups and glycerol backbone have proven to be more challenging, and large variation in performance with different force field occurs (16-19). Predictive power of MD simulations on lipid structure usually decreases close to the water–lipid interfacial region, and more attention for the modeling of this region has been put in lately (3, 20-22).

Atomistic MD simulations of membrane systems have been previously used to research the effects of changing different physiologically relevant conditions, such as the hydration level, and the ion concentrations (16, 23-27). Lower hydration is relevant in studying many biological processes, such as membrane fusion (28); ions are present in all biological systems, and ion–

membrane interactions are of a key importance e.g., in neuron studies (29-31). Experimental studies have shown that the phosphatidyl choline headgroup order parameters rise in response to lowering hydration and drop in response to cation binding (3). A good quality atomistic level force field should also capture these changes.

Response to lowering hydration level is qualitatively correctly produced by several current force fields; but large variation occurs in description of cation binding which is typically highly overestimated (16, 23). There are challenges in the correct description of Na^+ binding, but especially in the correct description of multivalent ions: Ca^{2+} over-accumulates at the membrane–water interface in most of the currently used force fields (18, 19, 23).

CHARMM36 is one of the most used lipid force fields; and as it performs quite well in most lipid studies, we use it here as a reference.

In this study we examined the performance of OPLS3e force field in membrane simulations. We demonstrate that OPLS3e produces C–H bond order parameters for POPC that are very close to experimental values and very similar when compared to the CHARMM36 forcefield. That said, in OPLS3e, as in many other force fields, the characterization of (especially of Ca^{2+}) ion binding to membrane seems problematic.

METHODS

Order parameters

In this work the C–H bond order parameters S_{CH} are used to assess the force field performance.

The S_{CH} depend on the angle θ between a C–H bond vector and membrane normal (in our simulations the z-axis direction) as

$$S_{\mathrm{CH}} = \frac{1}{2}\left\langle 3\cos^2\theta - 1 \right\rangle \qquad \text{(Eq. 1)}$$

where the angular brackets denote average over the sampled conformations. Order parameters from simulations can be calculated directly from the atomic coordinates using the Eq. 1.

Experimental order parameters can be determined for lipid C–H bonds with NMR techniques such as ^{2}H NMR (9) and ^{1}H-^{13}C NMR (10-12) using quadrupolar splitting and dipolar splitting, respectively. These methods are very accurate and highly sensitive to changes in the lipid structural ensemble (3). There are large amounts of experimental S_{CH} data available in the literature for different lipids measured with both ^{2}H and ^{13}C NMR, all in good agreement with each other (16). Experimental order parameters have been estimated to have at least +/- 0.02 accuracy (10, 16); the error range of 0.02 is used also in this study, as suggested by Botan et al. (16), as a sweet spot within which simulated order parameters should ideally reside compared to experimental data. Error range of 0.02 applies to magnitudes, but relative changes in S_{CH} can be measured with much higher accuracy if same equipment is used, allowing tracing of minor changes such as the response to lowering hydration or additional salt which is utilized also in this study (16, 23), for more discussion see Ref. (32)

Simulations

To compare the OPLS3e and CHARMM36 force fields to experimental data we performed equally long MD simulations (lengths ranging from 500 ns to 1μs) using both force fields with matching

hydration levels (Table 1) and salt concentrations (Table 2). Here we note just the key simulation details; all details are available in the run input files of the corresponding trajectories on Zenodo, see Tables 1 and 2 for the permanent links. Simulations used standard setup for planar bilayers, zero tension and periodic boundary conditions in either Desmond, implemented in Schrödinger suite package version 2019.4 (33, 34) (OPLS3e), or in GROMACS version 2019.5 (35) (CHARMM36). All simulated systems contained 200 POPC lipids (100 per leaflet) and they were generated using the system builder and the model system regeneration tools of the Schrödinger software suite and CHARMM-GUI Membrane builder, respectively. The NPT ensemble with temperature of 300 K and 1 atm pressure was used. In the simulations containing ions, ions were initially placed randomly in the water phase. Only the steady-state part of the simulations was analyzed, that is, after the bilayer area per lipid stabilized and (in salt-containing systems) no further ions accumulated in the membrane. Notably, the OPLS3e with high $CaCl_2$ concentration did not reach a steady state during 1μs, so the simulation was divided into 10x100 ns parts analyzed separately. Details of the simulations with varying hydration levels are shown in Table 1, and with varying concentrations of additional salt in Table 2.

Table 1. Simulated lipid bilayer systems with varying hydration levels. $N_{w/l}$ Water/lipid ratio, N_w Number of water molecules, t_{sim} Total simulation time, t_{anal} Time used for analysis, files Reference to simulation files

Forcefield	Lipid	$N_{w/l}$	N_w	t_{sim} (ns)	t_{anal} (ns)	files
OPLS3e (7)	POPC	44	8859	500	500	(36)
	POPC	20	4000	500	490	(37)
	POPC	10	2000	500	495	(38)
	POPC	5	1000	1000	600	(39)

CHARMM36 (40)	POPC	44	8880	500	460	(41)
	POPC	20	4000	500	400	(42)
	POPC	10	2000	500	425	(43)
	POPC	5	1000	1000	650	(44)

Table 2. Simulated lipid bilayer systems with varying concentration of additional salt. Salt concentrations are calculated as [salt] = $N_c \times$ [water]/N_w, where [water] is 55.5 M.

Forcefield for lipids/ions	Salt	[Salt] mM	N_w	N_c	t_{sim} (ns)	t_{anal} (ns)	link
OPLS3e (7)	NaCl	100	8880	16	1000	1000	(45, 46)
	NaCl	200	8880	32	1000	1000	(47, 48)
	NaCl	500	8880	80	1000	900	(49, 50)
	NaCl	1000	8880	160	1000	900	(51, 52)
	$CaCl_2$	50	8880	8	1000	500	(53, 54)
	$CaCl_2$	100	8880	16	1000	250	(55, 56)
	$CaCl_2$	200	8880	32	1000	10x100	(57, 58)
	$CaCl_2$	500	8880	80	1000	10x100	(59, 60)
	$CaCl_2$	1000	8880	160	1000	10x100	(61, 62)
CHARMM36/ Nbfix (40) (63)	NaCl	100	8880	16	500	475	(64)
	NaCl	200	8880	32	500	455	(65)
	NaCl	500	8880	80	500	440	(66)
	NaCl	1000	8880	160	500	485	(67)
	$CaCl_2$	50	8880	8	1000	850	(68)
	$CaCl_2$	100	8880	16	1000	850	(69)
	$CaCl_2$	200	8880	32	1000	750	(70)

$CaCl_2$	500	8880	80	1000	850	(71)
$CaCl_2$	1000	8726	158	1000	800	(72)

Starting structures and simulation details

OPLS3e

Starting structures were constructed using the system builder and model system regeneration tools implemented in the Schrödinger software package (33). The SPC water model (73) was used to solvate the systems. In addition, TIP3P (74) was used as a comparison in few systems to ensure that the water model does not significantly influence the order parameters (see Supplementary Information for details). For the dehydrated systems, excess water was removed from the starting structure of the full hydration system to attain the different hydration states. For the ion-containing systems, numbers of ions were calculated as $Nc = [salt] \times N_w / [water]$, where [water]=55.5 M. The system with the strongest ion concentration (1 M) was constructed first using the system builder, and other concentrations were generated by randomly removing excess ions. Simulations were performed using Desmond in Schrödinger suite's package version 2019-4 (33, 34). Default settings for membrane systems were used with 2 fs time step and saving data every 10 ps; systems were relaxed before simulations with the default membrane relaxation protocol of Desmond. Temperature was set at 300 K and the system was kept in the NPT ensemble with semi-isotropic Martyna–Tobias–Klein barostat (75) and the Nosé–Hoover chain thermostat (76).

CHARMM36

The starting structures were constructed using the CHARMM-GUI Membrane Builder (www.charmm-gui.org) (77). CHARMM TIP3P water model (78, 79) was used to solvate the systems. Different hydration states were generated by removing excess water from the systems.

Ions were added by using `gmx genion` tool in the GROMACS software package (35). All simulations were performed with GROMACS version 2019.5 (35). Force field parameters were taken as in the CHARMM-GUI outputs; consequently, the Nbfix parameters (63) were used for ions. Simulations were performed with 2 fs time step and data saved every 10 ps. Temperature of 300 K was maintained with the Nosé–Hoover thermostat(80, 81), and semi-isotropic Parrinello–Rahman barostat (82) was used to control the pressure.

Analysis

The S_{CH} were calculated directly using the Eq (1). The S_{CH} of each C–H bond was gained by calculating first the S_{CH} of each individual lipid over time separately, and then calculating the average and the standard error of mean over different lipids. This analysis was performed using the Python program calcOrderParameters.py from NMRlipids github (83). The program uses the MDAnalysis library (84, 85). Number densities were obtained by using the `gmx density` tool in GROMACS software package (35). Desmond files were converted for analysis into GROMACS format using VMD (86) for trajectories and convert.py by Intermol (87) for other files. After convert.py conversion, names of the waters and ions, and individual representation of ions were manually modified to match the other files.

RESULTS AND DISCUSSION

We calculated the C–H bond order parameters S_{CH}, see Eq. (1), from the simulations performed at different conditions, see Tables 1 and 2, with OPLS3e and CHARMM36 force fields and compared them to the experimental S_{CH} available in the literature.

Full hydration

Most S_{CH} produced by OPLS3e reside within ±0.02 from the experimental values, that is, within the estimated error range of NMR experiments (Fig. 2). However, problems with S_{CH} magnitude occur in g_1, near double bond of the sn-2 chain (C9) and at the start of sn-1 chain. For these regions the experimental error range is not reached with either of the force fields. Whereas OPLS3e and CHARMM36 produce almost identical S_{CH} for headgroup and glycerol backbone, the performance of OPLS3e for acyl chain regions seems to surpass CHARMM36.

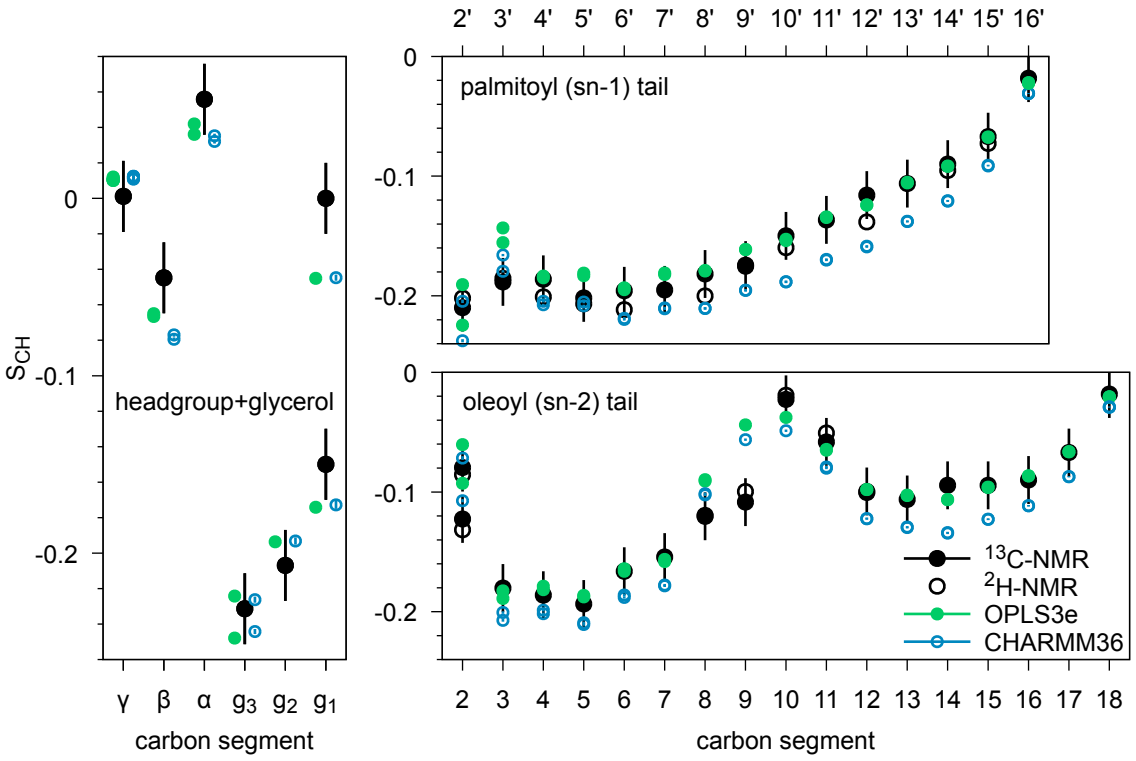

Figure 2. Carbon–hydrogen bond order parameters S_{CH} at full hydration for headgroup, backbone, and acyl chains in simulations and experiments. Experimental values for the POPC ^{1}H- ^{13}C NMR at 300 K are from Ref. 12 and ^{2}H-NMR are from Ref. 88. The +/- 0.02 error bars of the ^{13}C experimental values represent also the range within which most of the published experimental data resides, see discussion in text. For naming of carbon segments, see Fig. 1.

In addition to magnitudes, a high-fidelity simulation model should produce correct forking pattern of S_{CH}. The term forking is used to describe occurrence of unequal S_{CH} for different hydrogens attached to the same carbon, indicating different orientational populations of the two C–H bonds. It has been shown to not result from two separate population of lipids (89, 90). Based on experimental data, most carbons of POPC have equally sampled C–H bond orientations and produce equal S_{CH} for both hydrogens; but there are few exceptions: the R and S hydrogens attached to the g_1 and g_3 carbons (12, 89) in the glycerol backbone show in experiments significant and moderate forking, respectively, and the C2 carbon of sn-2 chain shows moderate forking, see Fig 2. An accurate forcefield should produce correct forking for g_1, g_3, and C2—but show no forking for other carbons. Forking is illustrated in the Fig. 3 by angle distributions towards membrane normal. In CHARMM36 at full hydration, angle distributions for both hydrogens attached to the α carbon are equal (Fig. 3A), but at 5 w/l (Fig. 3B) distributions are unequal showing forking.

At full hydration, OPLS3e and CHARMM36 correctly produce forking for g_1 and g_3, and C2 of sn-2 chain. The C2 of sn-2 chain is of particular interest, as several force fields have been shown to struggle in this area (3, 17). However, both force fields produce forking for C2 and C3 at the start of sn-1 chain, which is not in agreement with the experimental data.

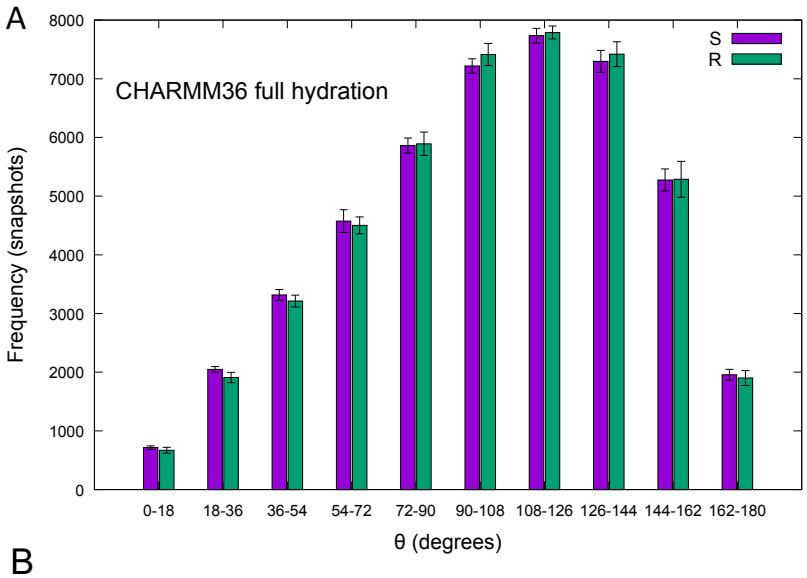
A
CHARMM36 full hydration
S
R
Frequency (snapshots)
0
1000
2000
3000
4000
5000
6000
7000
8000
0-18
18-36
36-54
54-72
72-90
90-108
108-126
126-144
144-162
162-180
θ (degrees)

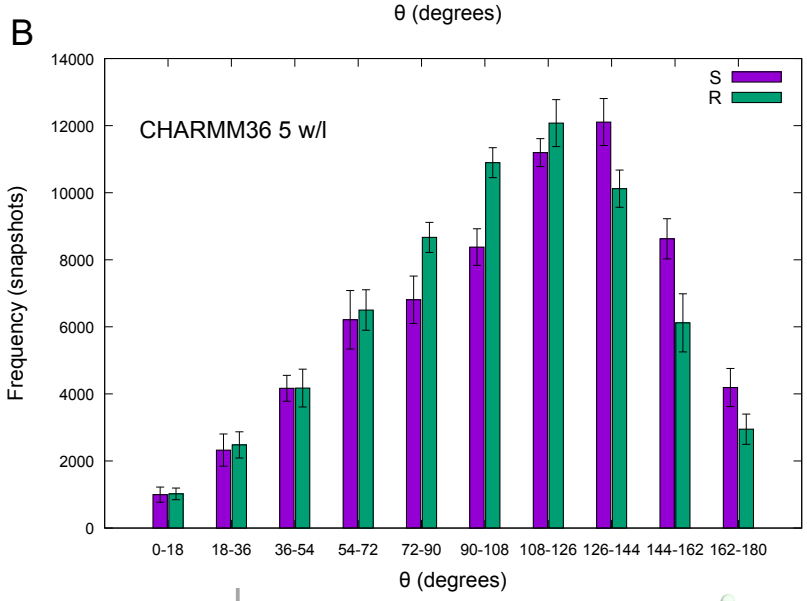
B
CHARMM36 5 w/l
S
R
Frequency (snapshots)
0
2000
4000
6000
8000
10000
12000
14000
0-18
18-36
36-54
54-72
72-90
90-108
108-126
126-144
144-162
162-180
θ (degrees)

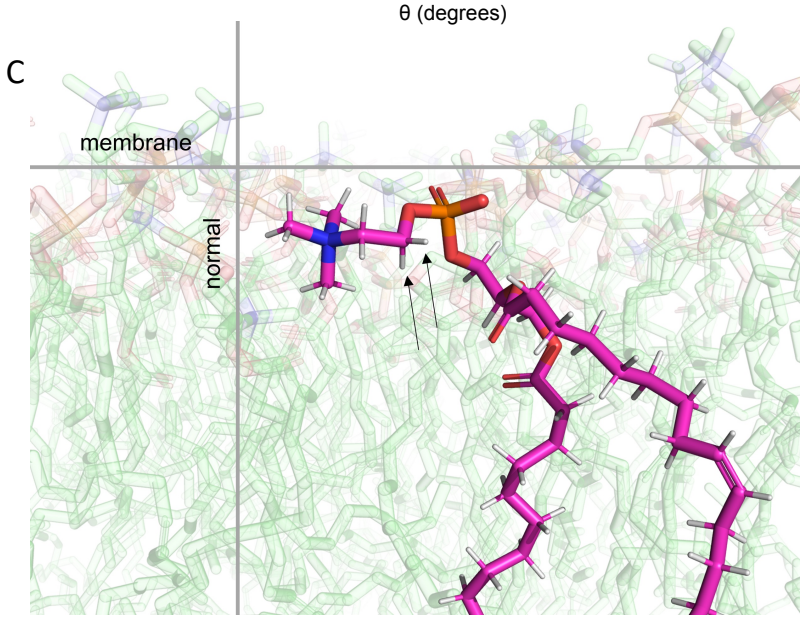
C
membrane
normal

Figure 3. Illustration of forking. The θ-angle distribution of the α-carbon C–H bonds for R and S hydrogens (A) in CHARMM36 at full hydration (44 w/l) showing no forking and (B) in CHARMM36 at 5 w/l showing forking, cf. Fig 4. Distributions are calculated over 5 lipids as an example, error bars representing standard error of means. θ is the angle between a C–H bond and the membrane normal, see Methods for more information (C) A snapshot with the α-carbon hydrogens marked with arrows.

In general, OPLS3e produces very similar pattern of order parameters at full hydration as CHARMM36: close to experimental values but not within experimental accuracy. However, both force fields have problems with the correct description of g_1 at glycerol backbone, the beginning of the acyl tails, and the double bond of oleoyl chain. Therefore, we can conclude that OPLS3e produces comparable S_{CH} to CHARMM36 at full hydration, suggesting that structural description of POPC is similar and reasonably accurate in these force fields.

Dehydration

To examine how decreasing hydration affects the performance of OPLS3e, we compared the headgroup order parameters S^{β}_{CH} and S^{α}_{CH} from OPLS3e and CHARMM36 simulations against experimental NMR data (Fig. 4). In experiments, S^{β}_{CH} and S^{α}_{CH} rise when hydration level drops, a change that should be captured in simulations. Although the S^{β}_{CH} are not within +/- 0.02 from experimental data (Fig. 4), which indicates that neither force field exactly produces the atomistic resolution structural ensemble of the headgroup, the changes produced in S^{β}_{CH} and S^{α}_{CH} are qualitatively in line with experimental data: Both increase as hydration level decreases in OPLS3e, and in CHARMM36. Also, the magnitude of the rise for S^{α}_{CH} in OPLS3e aligns with the

experimentally measured rise, but for S^{β}_{CH} the rise is exaggerated. Similar observations can be made with CHARMM36; however, an additional forking not reported in previous studies is occurring in CHARMM36 at the low hydration level of 5 w/l, see Figs. 3 and 4. Our simulation length at 5 w/l (1000 ns, see Table 1) was reasonably long compared to earlier simulation studies reporting S^{β}_{CH} and S^{α}_{CH} at low hydration (16), resulting in small error estimates and making the difference between the C–H bonds clearly visible.

Based on these data, structural response to dehydration seems quite realistic for the headgroup in OPLS3e. Botan et al. suggest an intuitive explanation for the rising headgroup order parameters of the headgroup to be the choline headgroup orientating more parallel to the membrane as the interlamellar space shrinks in response to a decreasing hydration level (16). To conclude: in response to dehydration, OPLS3e does not produce atomistic resolution but its performance is very similar to CHARMM36 and headgroup orientation in OPLS3e can be thought to be reasonably accurate under dehydrated conditions. Although, many currently available force fields produce qualitatively correct response to lowering hydration, OPLS3e and CHARMM36 seem to be among the most realistic considering the magnitude of the response.

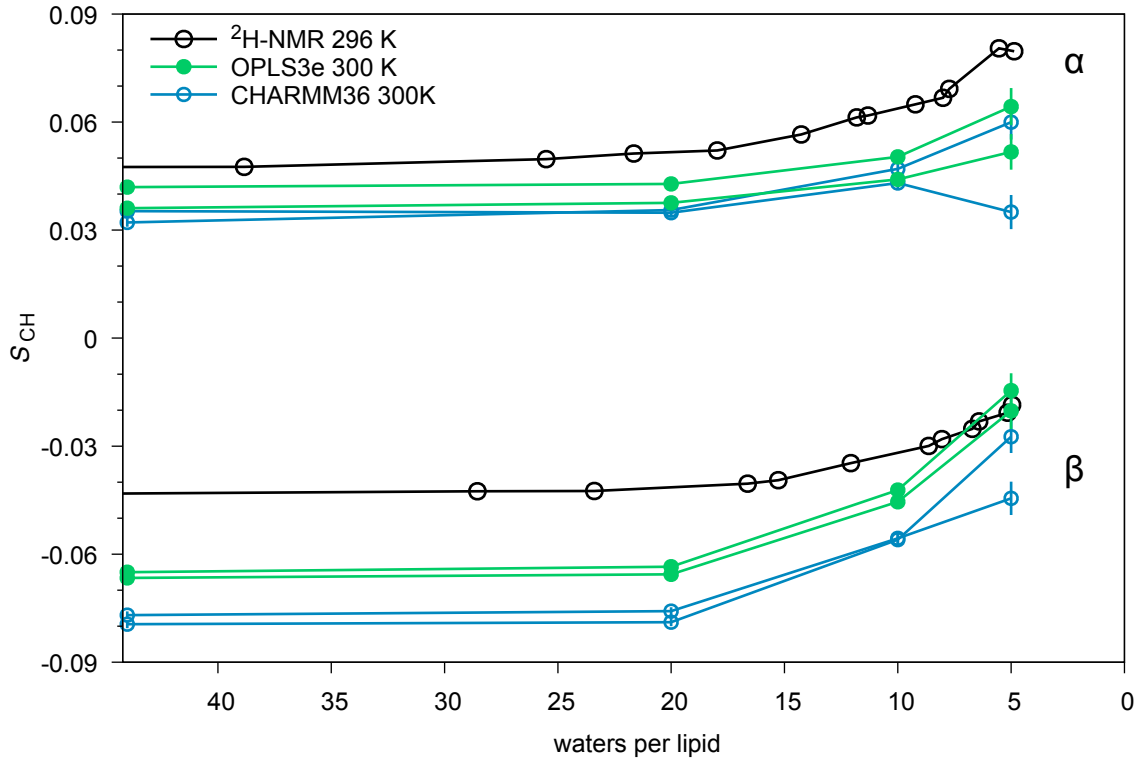

Figure 4. Response of the headgroup S^{β}_{CH} and S^{α}_{CH} order parameters to decreasing hydration level for the headgroup α and β. Experimental values for POPC (^{2}H NMR) at 296 K are from Ref. 91. Notably, small changes in temperature seem not to have major effect on S_{CH}, see SI Figs. 10 and 11.

Ions

Order parameters of phosphatidylcholine (PC) headgroup C–H bonds can be used to compare ion binding to lipid membranes in experiments and simulations (23). Charged objects on a PC bilayer interface induce systematic changes for the order parameters of the α and β carbons: Positive charge induces a decrease, and negative charge an increase in S^{β}_{CH} and S^{α}_{CH}. The concept, often referred to as the "molecular electrometer", has a strong experimental background (92) and Catte et al. (23) have demonstrated that also in atomistic MD simulations, the S^{β}_{CH} and S^{α}_{CH} act as indicator for bound cations. Therefore, comparison of ion affinities between experiments and

simulations based on the PC headgroup order parameters is possible, and allows the assessment of the simulation model quality at different salt concentrations.

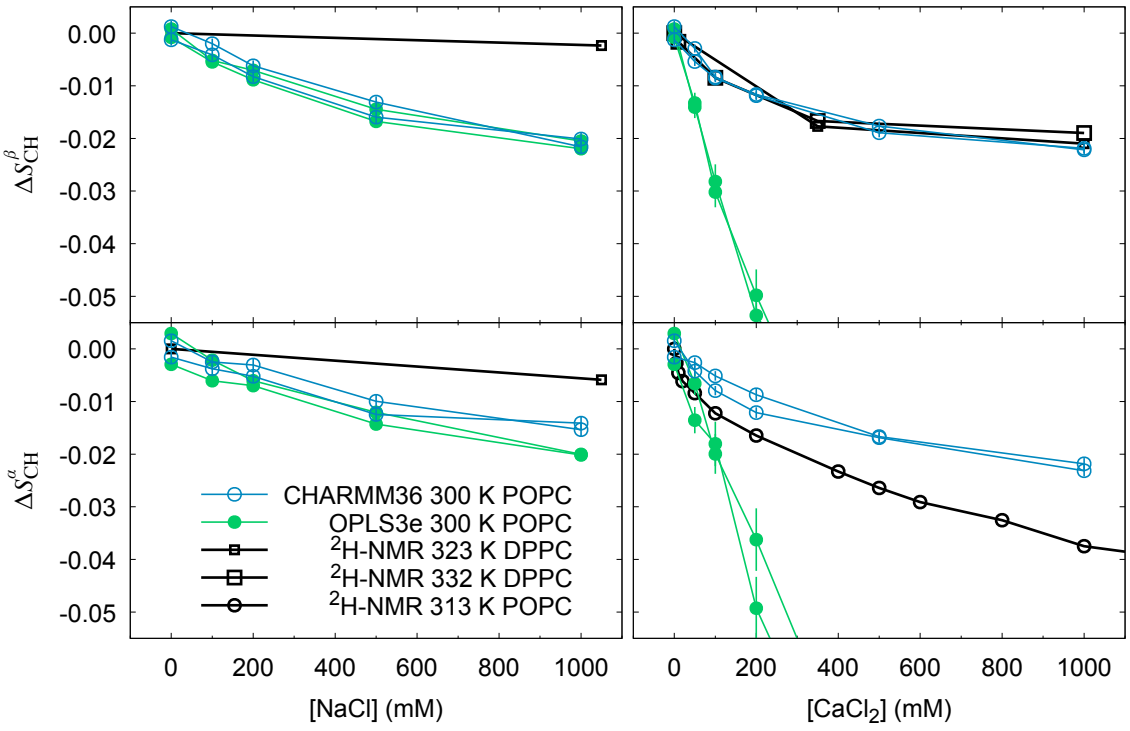

Figure 5. Change of order parameters in the headgroup α (lower panels) and β (upper panels) segments in response to rising concentrations of NaCl (left panels) or $CaCl_2$ (right panels). Experimental values for DPPC (^{2}H NMR) at 323 K and 332 K are from Ref. 93 and for POPC (^{2}H NMR) at 313 K are from Ref. 94. The out-of-bounds ΔS^{β}_{CH} points of OPLS3e in response to $CaCl_2$ (top right panel) are -0.102±0.0085 and -0.089±0.0090 (500 mM), and -0.13±0.011 and -0.11±0.013 (1000 mM). Corresponding values for ΔS^{α}_{CH} (bottom right panel) are -0.10±0.010 and -0.093±0.010 (500 mM), and -0.073±0.016 and -0.097±0.015 (1000 mM). Full figure is available in the SI (SI Fig 3). Due to their very slow equilibration (see Fig. SI 4), for the OPLS3e $CaCl_2$ 200, 500 and 1000 mM concentrations, the last 100 ns of the 1 μs simulation was used here. Note that to show possible forking at [salt] = 0, best seen in the bottom left panel for the OPLS3e, the average of the C–H bond order parameters of the R and S hydrogens was used to set the baseline.

In the experiments, adding NaCl induces minimal decrease to S^{α}_{CH} and $S^{\beta}_{CH,}$ suggesting minimal Na^+ binding to membrane (93). Several MD force fields overestimate Na^+ binding, and consequently S^{α}_{CH} and S^{β}_{CH} drop significantly more than in the experiments (23). Based on the headgroup order parameter change (Fig. 5 left panels) and ion distributions (Fig. 6) in our simulations, OPLS3e is not an exception: Na^+ binding is overestimated. Notable is that overestimation is visible also at lower concentrations, near the physiological 150 mM concentration, that has the highest relevance in life sciences. Shapes of the order parameter curves in response to rising concentration of NaCl are very similar in OPLS3e and CHARMM36 (Fig. 5 left panels). Also, distributions of Na^+ and Cl^- seem highly similar (Fig 6), which suggests similar response to rising concentrations of NaCl in both force fields. For CHARMM36 we have included the non-bonded fix (NBFix) corrections for ion parameters that have been suggested to recover overestimation of Na^+ binding (95); however, the NbFix-corrected CHARMM36 still appears to overestimate Na^+ binding (Fig 5. left panels).

Distributions of Na^+ and Cl^- (Fig. 6) show that at lower salt concentrations (100 and 200 mM) ions are not only accumulated in the vicinity of the membrane, but they are also unevenly distributed in the bulk solution (Na^+ and Cl^- curves do not converge in the bulk); meaning that even with the rather large water/lipid ratios used here, the desired effect of having equal concentrations of both ions in the bulk solution is not reached in either of the forcefields with [NaCl] < 500 mM.

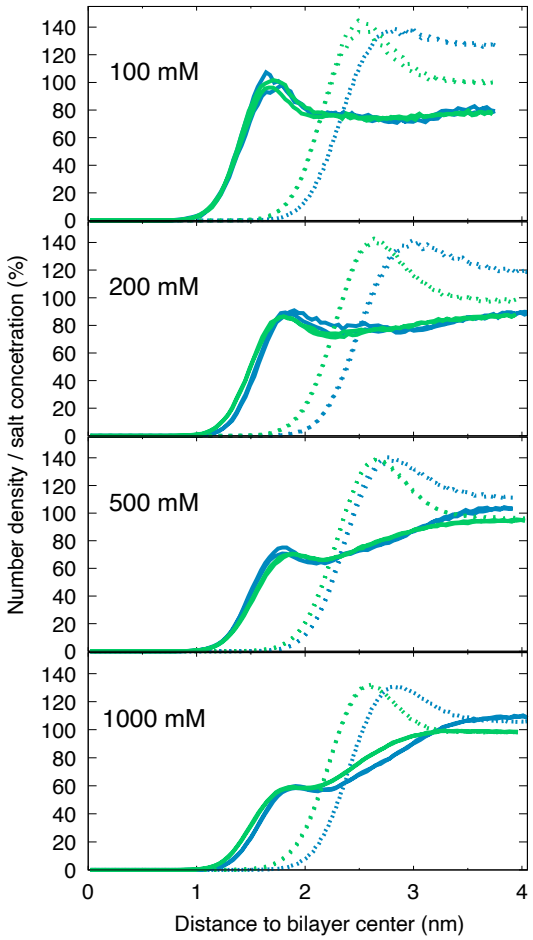

Figure 6. Distribution for Na^+ (solid lines) and Cl^- (dashed lines) ions along the bilayer normal shown as percentage of salt concentration. Green represents OPLS3e and blue CHARMM36. The graphs were obtained by dividing the number densities with the total salt concentration. Note that both leaflets are plotted (two almost fully overlapping lines), to highlight the symmetry of the ion distributions.

Contrary to Na^+ ions, divalent Ca^{2+} ions bind significantly to lipid bilayers in experiments and the PC headgroup order parameters decrease when $CaCl_2$ concentration increases. Correct description of calcium binding to bilayers has proven to be challenging and it seems that only the ECC-POPC model of the current force fields produces the quantitatively accurate response (18,

23, 27). However, many force fields can have qualitatively right response to Ca^{2+}; but overestimate the binding affinity. OPLS3e too produces qualitatively right order parameter response to Ca^{2+} ions: S^{β}_{CH} and S^{α}_{CH} decrease with rising concentration of Ca^{2+}; but the decrease of is far too great (Fig. 5 right panels) and binding of Ca^{2+} is highly overestimated (Fig. 7). Order parameters of CHARMM36 are closer to experimental data than OPLS3e, suggesting that OPLS3e produces poorer response to additional $CaCl_2$ than the CHARMM36 forcefield. However, S^{α}_{CH} of CHARMM36 suggest slight underestimation of Ca^{2+} binding, and the NaCl and $CaCl_2$ responses seem very much alike, suggesting that, as already previously indicated in the SI of Ref. (18), CHARMM36 with NbFix parameters does not distinguish the difference between monovalent Na^{+} and divalent Ca^{2+} seen in the experiments.

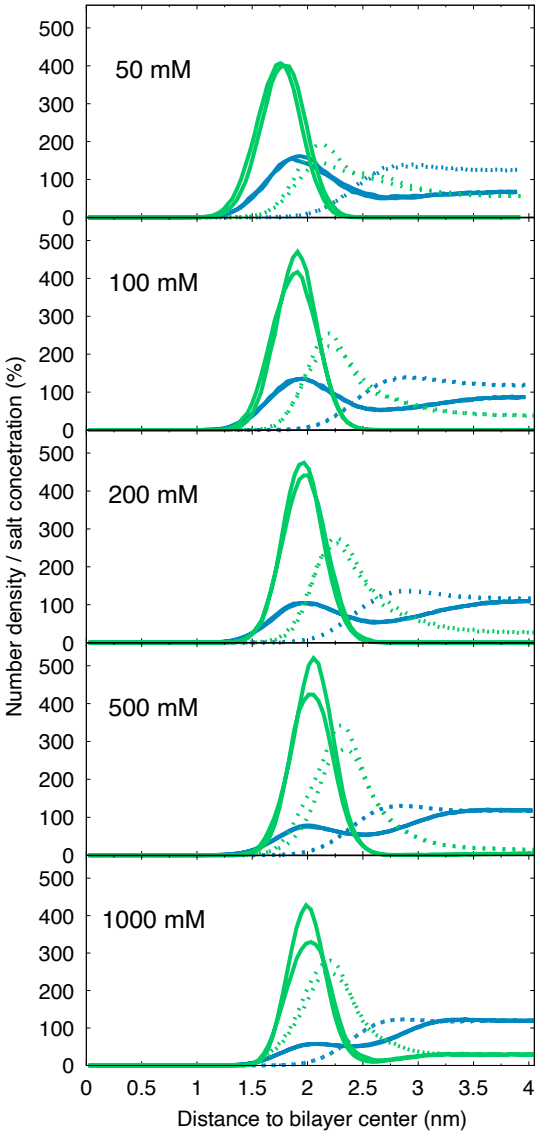

Figure 7. Distribution for Ca^{2+} (solid lines) and Cl^- (dashed lines) ions along the bilayer normal shown as percentage of salt concentration. Green represents OPLS3e and blue CHARMM36. The graphs were obtained by dividing the number densities with the total salt concentration. Due to their very slow equilibration (see Fig. SI 4), of the OPLS3e $CaCl_2$ 200, 500, and 1000 mM concentrations, the last 100 ns of the 1 μs simulation was used here. Note that both leaflets are plotted (two almost fully overlapping lines).

Overestimation of ion binding in OPLS3e can be seen also in ion distributions, especially for $CaCl_2$ (Fig. 7). Membrane pulls all calcium ions from the solution at low (≤ 200 mM) concentrations (and nearly all at higher concentrations), leaving no Ca^{2+} ions to the bulk. A high density of Ca^{2+} ions can be seen at the membrane surface, and consequently, the neutral PC bilayer will appear as positively charged, pulling a high density of Cl^- ions next to the Ca^{2+}. This charge layering will result in a strong electrostatic gradient. Such an artificially charged membrane can distort MD simulation results; in addition to effects on membrane behavior, influence on charged domains of membrane proteins is also conceivable, and might underlie some contradicting MD simulation results (96, 97). Therefore, extreme caution should be exercised when simulating membrane protein systems containing ions using force fields that are known to overestimate cation binding.

It is worth keeping in mind that as calcium binding of OPLS3e is so highly overestimated that (nearly) all Ca^{2+} is bound to bilayer, and no Ca^{2+} is left to solution, studying effects of calcium solutions on systems containing membranes using OPLS3e will be very difficult.

To conclude, additional NaCl produces similar response in both OPLS3e and CHARMM36: Slight overestimation of sodium binding compared to the minimal binding suggested by experimental data. On the contrary, responses to $CaCl_2$ differ in our MD simulation between OPLS3e and CHARMM36. OPLS3e produces qualitatively right response to rising $CaCl_2$ concentration, but radically overestimates the Ca^{2+} binding. Response of CHARMM36 seem to be closer to the experiments, although it is not able to reproduce the difference between Na^+ and Ca^{2+} ions. The commonly occurring overestimation of cation binding poses one of the biggest problems

in current membrane modeling using MD simulations as it may result in positively charged membrane which can qualitatively distort the results.

Several strategies to fix the over binding of ions to membranes have been proposed in the literature. Nbfix, which was used for CHARMM36 in this study, addresses the issue by tuning non-bonded parameters for specific atom pairs separately instead of using the standard arithmetic combining rule (63). Another alternative solution is the electronic continuum correction (ECC) strategy which takes electronic polarization effects of solvent into account by scaling the charge of the ions (24, 27). We tested a similar scaling as in the ECC model for NaCl and $CaCl_2$ in OPLS3e, which pre-scaling to overestimates Na^+ and Ca^{2+} binding to membrane (Fig 5.). Scaling of 0.75 for Na^+ and Cl^- ions decreased Na^+ binding to membrane, and order parameters were closer to experimental values than without scaling (SI Fig. 6). For $CaCl_2$, the similar simple scaling of ionic charges did not fix the surplus ion binding to the membrane (SI Figs 7 and 8). In ECC-POPC model (27) scaling of both ions and partial charges of lipid head group atoms was conducted resulting in one of the most realistic force fields for lipids so far, since it can produce accurate binding also for divalent Ca^{2+} which, as already previously stated, has been very challenging with all current force fields.

For both force fields used in this study, OPLS3e and CHARMM36, new releases have been published recently. OPLS4 was published in 2021, with updates, e.g., on the representation of hydration and treatment of molecular ions (98). There were no changes in membrane parametrization. New CHARMM36 parameters called as C36/LJ-PME were also published in 2021 (20). Parameters have been optimized for lipid membranes with semi-automated approach

including long-range dispersion using Lennard-Jones particle-mesh Ewald (LJ-PME) approach (20). Order parameters were used as one of the optimization targets and based on their study, order parameters for head group and tails of DPPC and DMPC lipids at full hydration align quite well with the experimental data. It will be interesting to see if these new updates offer improved performance for membranes especially in the presence of ions which has been challenging area to be simulated correctly by the earlier force fields.

CONCLUSIONS

MD simulations using accurate force fields allow studying biomembranes at different conditions to interpret experimental results and to get knowledge of membrane structure and the function, and dynamics of membrane-bound proteins. Here we demonstrate the performance of OPLS3e to be reasonably accurate for POPC membranes at full hydration and upon dehydration: The C–H bond order parameters produced with OPLS3e behave similarly to the well-established membrane force field CHARMM36 and closely follow the experimental observations. However, extreme caution should be exercised with systems containing ions, especially Ca^{2+} ions: OPLS3e, similarly to most other force fields, overestimates the binding of the cationic ions to the membrane which both disrupts the neutral net charge of the membrane surface and changes the concentration of ions in the surrounding solvent. These issues could affect, for example, the structure and dynamics of the charged domains of membrane-bound proteins in unexpected ways.

Our results confirm that OPLS3e can be used for reliable MD simulations with simple POPC bilayers. Future studies should elucidate its performance with more diverse bilayers, such as ones containing mixtures of different lipids or cholesterol.

Data and Software Availability

The scripts for the bond order parameter analysis are freely available at NMRlipids GitHub (https://github.com/NMRLipids) and the analyzed trajectories are permanently freely available at Zenodo (https://zenodo.org/).

Author Contributions

AP, PB, and MSM came up with the research idea. ML conducted the simulations and analysis under the supervision of AP, PB, and MSM. All authors contributed to the writing of the manuscript and have given approval to the final version of the manuscript. ‡These authors contributed equally.

Funding Sources

ML, AP, and PB received funding from Finnish Cultural Foundation, The UEF Doctoral Programme, and competitive funding to strengthen university research profiles, 5th call, funding to University of Eastern Finland, funded by the Academy of Finland, funding decision nro 325022.

ACKNOWLEDGMENTS

The authors thank CSC – IT Center for Science, Finland, for computational resources.

REFERENCES

References

1. van Meer G, Voelker DR, Feigenson GW. Membrane lipids: where they are and how they behave. Nature reviews. Molecular cell biology. 2008 Feb;9(2):112-24.

2. Penke B, Paragi G, Gera J, Berkecz R, Kovács Z, Crul T, et al. The Role of Lipids and Membranes in the Pathogenesis of Alzheimer's Disease: A Comprehensive View. Curr Alzheimer Res. 2018;15(13):1191-212.

3. Ollila OHS, Pabst G. Atomistic resolution structure and dynamics of lipid bilayers in simulations and experiments. Biochimica et Biophysica Acta (BBA) - Biomembranes. 2016 October 1,;1858(10):2512-28.

4. Wanderlingh U, Branca C, Crupi C, Conti Nibali V, La Rosa G, Rifici S, et al. Molecular Dynamics of POPC Phospholipid Bilayers through the Gel to Fluid Phase Transition: An Incoherent Quasi-Elastic Neutron Scattering Study. Journal of Chemistry. 2017 /10/08;2017:e3654237.

5. Dauber-Osguthorpe P, Hagler AT. Biomolecular force fields: where have we been, where are we now, where do we need to go and how do we get there? J Comput Aided Mol Des. 2019 -02;33(2):133-203.

6. Lyubartsev AP, Rabinovich AL. Force Field Development for Lipid Membrane Simulations. Biochimica et Biophysica Acta (BBA) - Biomembranes. 2016 October 1,;1858(10):2483-97.

7. Roos K, Wu C, Damm W, Reboul M, Stevenson JM, Lu C, et al. OPLS3e: Extending Force Field Coverage for Drug-Like Small Molecules. J Chem Theory Comput. 2019 Mar 12,;15(3):1863-74.

8. Harder E, Damm W, Maple J, Wu C, Reboul M, Xiang JY, et al. OPLS3: A Force Field Providing Broad Coverage of Drug-like Small Molecules and Proteins. J Chem Theory Comput. 2016 Jan 12,;12(1):281-96.

9. Seelig J. Deuterium magnetic resonance: theory and application to lipid membranes. Q Rev Biophys. 1977 Aug;10(3):353-418.

10. Gross JD, Warschawski DE, Griffin RG. Dipolar Recoupling in MAS NMR: A Probe for Segmental Order in Lipid Bilayers. J Am Chem Soc. 1997 -01-01;119(4):796-802.

11. Dvinskikh SV, Castro V, Sandström D. Efficient solid-state NMR methods for measuring heteronuclear dipolar couplings in unoriented lipid membrane systems. Phys Chem Chem Phys. 2005 Feb 21,;7(4):607-13.

12. Ferreira TM, Coreta-Gomes F, Ollila OHS, Moreno MJ, Vaz WLC, Topgaard D. Cholesterol and POPC segmental order parameters in lipid membranes: solid state 1H–13C NMR and MD simulation studies. Phys Chem Chem Phys. 2013 -01-16;15(6):1976-89.

13. Klauda JB, Venable RM, Freites JA, O'Connor JW, Tobias DJ, Mondragon-Ramirez C, et al. Update of the CHARMM all-atom additive force field for lipids: validation on six lipid types. J Phys Chem B. 2010 -06-17;114(23):7830-43.

14. Jämbeck JPM, Lyubartsev AP. Derivation and systematic validation of a refined all-atom force field for phosphatidylcholine lipids. J Phys Chem B. 2012 -03-15;116(10):3164-79.

15. Dickson C, J., Madej BD, Skjevik ÅA, Betz RM, Teigen K, et al. Lipid14: The Amber Lipid Force Field. J Chem Theory Comput. 2014 -02-11;10(2):865-79.

16. Botan A, Favela-Rosales F, Fuchs PFJ, Javanainen M, Kanduč M, Kulig W, et al. Toward Atomistic Resolution Structure of Phosphatidylcholine Headgroup and Glycerol Backbone at Different Ambient Conditions. J Phys Chem B. 2015 Dec 10,;119(49):15075-88.

17. Pezeshkian W, Khandelia H, Marsh D. Lipid Configurations from Molecular Dynamics Simulations. Biophys J. 2018 -04-24;114(8):1895-907.

18. Antila H, Buslaev P, Favela-Rosales F, Ferreira TM, Gushchin I, Javanainen M, et al. Headgroup Structure and Cation Binding in Phosphatidylserine Lipid Bilayers. J Phys Chem B. 2019 -10-31;123(43):9066-79.

19. Bacle A, Buslaev P, Garcia-Fandino R, Favela-Rosales F, Mendes Ferreira T, Fuchs PFJ, et al. Inverse Conformational Selection in Lipid-Protein Binding. J Am Chem Soc. 2021 -09-01;143(34):13701-9.

20. Yu Y, Krämer A, Venable RM, Simmonett AC, MacKerell AD, Klauda JB, et al. Semi-automated Optimization of the CHARMM36 Lipid Force Field to Include Explicit Treatment of Long-Range Dispersion. J Chem Theory Comput. 2021 March 9,;17(3):1562-80.

21. Dickson CJ, Walker RC, Gould IR. Lipid21: Complex Lipid Membrane Simulations with AMBER. J Chem Theory Comput. 2022 -03-08;18(3):1726-36.

22. Grote F, Lyubartsev AP. Optimization of Slipids Force Field Parameters Describing Headgroups of Phospholipids. J Phys Chem B. 2020 -10-08;124(40):8784-93.

23. Catte A, Girych M, Javanainen M, Loison C, Melcr J, Miettinen MS, et al. Molecular electrometer and binding of cations to phospholipid bilayers. Phys Chem Chem Phys. 2016 Nov 30,;18(47):32560-9.

24. Kohagen M, Mason PE, Jungwirth P. Accounting for Electronic Polarization Effects in Aqueous Sodium Chloride via Molecular Dynamics Aided by Neutron Scattering. J Phys Chem B. 2016 -03-03;120(8):1454-60.

25. Melcrová A, Pokorna S, Pullanchery S, Kohagen M, Jurkiewicz P, Hof M, et al. The complex nature of calcium cation interactions with phospholipid bilayers. Sci Rep. 2016 -12-01;6:38035.

26. Javanainen M, Melcrová A, Magarkar A, Jurkiewicz P, Hof M, Jungwirth P, et al. Two cations, two mechanisms: interactions of sodium and calcium with zwitterionic lipid membranes. Chem Commun (Camb). 2017 -05-11;53(39):5380-3.

27. Melcr J, Martinez-Seara H, Nencini R, Kolafa J, Jungwirth P, Ollila OHS. Accurate Binding of Sodium and Calcium to a POPC Bilayer by Effective Inclusion of Electronic Polarization. J Phys Chem B. 2018 April 26,;122(16):4546-57.

28. Knecht V, Marrink S. Molecular Dynamics Simulations of Lipid Vesicle Fusion in Atomic Detail. Biophysical journal. 2007;92(12):4254-61.

29. Kavalali ET. The mechanisms and functions of spontaneous neurotransmitter release. Nat Rev Neurosci. 2015 -01;16(1):5-16.

30. Magarkar A, Jurkiewicz P, Allolio C, Hof M, Jungwirth P. Increased Binding of Calcium Ions at Positively Curved Phospholipid Membranes. J Phys Chem Lett. 2017 -01-19;8(2):518-23.

31. Flood E, Boiteux C, Lev B, Vorobyov I, Allen TW. Atomistic Simulations of Membrane Ion Channel Conduction, Gating, and Modulation. Chem Rev. 2019 -07-10;119(13):7737-832.

32. Ollila S, Miettinen MS, Vogel A. Accuracy of order parameter measurements, 2015. DOI: 10.6084/m9.figshare.1577576. The NMRLipids collaboration.

33. Schrödinger Release 2020-4: Maestro, Schrödinger, LLC, New York, NY, 2020. Maestro.

34. Bowers KJ, Chow E, Xu H, Dror RO, Eastwood MP, Gregersen BA, Klepeis JL, Kolossvary I, Moraes MA, Sacerdoti FD, Salmon JK, Shan Y, and Shaw DE. Scalable Algorithms for Molecular Dynamics Simulations on Commodity Clusters. ; 2006, November.

35. Abraham M, Murtola T, Schulz R, Páll S, Smith JC, Hess B, et al. GROMACS: High performance molecular simulations through multi-level parallelism from laptops to supercomputers. . 2015.

36. Lindström M. MD simulation of POPC bilayer with OPLS3e force field. Full hydration 44 w/l. 2022, DOI: 10.5281/zenodo.6342807.

37. Lindström M. MD simulation of POPC bilayer with OPLS3e force field. 20 w/l. 2022, DOI: 10.5281/zenodo.6345186.

38. Lindström M. MD simulation of POPC bilayer with OPLS3e force field. 10 w/l. 2022, DOI: 10.5281/zenodo.6345702.

39. Lindström M. MD simulation of POPC bilayer with OPLS3e force field. 5 w/l. 2022, DOI: 10.5281/zenodo.6345780.

40. Klauda JB, Venable RM, Freites JA, O'Connor JW, Tobias DJ, Mondragon-Ramirez C, et al. Update of the CHARMM all-atom additive force field for lipids: validation on six lipid types. J Phys Chem B. 2010 Jun 17,;114(23):7830-43.

41. Lindström M. MD simulation of POPC bilayer with CHARMM36 force field. Full hydration 44 w/l. 2022, DOI: 10.5281/zenodo.6336691.

42. Lindström M. MD simulation of POPC bilayer with CHARMM36 force field. 20 w/l. 2022, DOI: 10.5281/zenodo.6335769.

43. Lindström M. MD simulation of POPC bilayer with CHARMM36 force field. 10 w/l. 2022, DOI: 10.5281/zenodo.6334005.

44. Lindström M. MD simulation of POPC bilayer with CHARMM36 force field. 5 w/l. 2022, DOI: 10.5281/zenodo.6333548.

45. Lindström M. MD simulation of POPC bilayer with OPLS3e force field, 100 mM NaCl part 1. 2022, DOI: 10.5281/zenodo.6355375.

46. Lindström M.MD simulation of POPC bilayer with OPLS3e force field, 100 mM NaCl part 2. 2022, DOI: 10.5281/zenodo.6361140.

47. Lindström M. MD simulation of POPC bilayer with OPLS3e force field, 200 mM NaCl part 1. 2022, DOI: 10.5281/zenodo.6361725.

48. Lindström M. MD simulation of POPC bilayer with OPLS3e force field, 200 mM NaCl part 2. 2022, DOI: 10.5281/zenodo.6363524.

49. Lindström M. MD simulation of POPC bilayer with OPLS3e force field, 500 mM NaCl part 1. 2022, DOI: 10.5281/zenodo.6364216.

50. Lindström M. MD simulation of POPC bilayer with OPLS3e force field, 500 mM NaCl part 2. 2022, DOI: 10.5281/zenodo.6364498.

51. Lindström M. MD simulation of POPC bilayer with OPLS3e force field, 1000 mM NaCl part 1. 2022, DOI: 10.5281/zenodo.6365067.

52. Lindström M. MD simulation of POPC bilayer with OPLS3e force field, 1000 mM NaCl part 2. 2022, DOI: 10.5281/zenodo.6366287.

53. Lindström M. MD simulation of POPC bilayer with OPLS3e force field, 50 mM CaCl2 part 1. 2022, DOI: 10.5281/zenodo.6345943.

54. Lindström M. MD simulation of POPC bilayer with OPLS3e force field, 50 mM CaCl2 part 2. 2022, DOI: 10.5281/zenodo.6346717.

55. Lindström M. MD simulation of POPC bilayer with OPLS3e force field, 100 mM CaCl2 part 1. 2022, DOI: 10.5281/zenodo.6347738.

56. Lindström M. MD simulation of POPC bilayer with OPLS3e force field, 100 mM CaCl2 part 2. 2022, DOI: 10.5281/zenodo.6347982.

57. Lindström M. MD simulation of POPC bilayer with OPLS3e force field, 200 mM CaCl2 part 1. 2022, DOI: 10.5281/zenodo.6348436.

58. Lindström M. MD simulation of POPC bilayer with OPLS3e force field, 200 mM CaCl2 part 2. 2022, DOI: 10.5281/zenodo.6350600.

59. Lindström M. MD simulation of POPC bilayer with OPLS3e force field, 500 mM CaCl2 part 1. 2022, DOI: 10.5281/zenodo.6350923.

60. Lindström M. MD simulation of POPC bilayer with OPLS3e force field, 500 mM CaCl2 part 2. 2022, DOI: 10.5281/zenodo.6351089.

61. Lindström M. MD simulation of POPC bilayer with OPLS3e force field, 1000 mM CaCl2 part 1. 2022, DOI: 10.5281/zenodo.6351349.

62. Lindström M. MD simulation of POPC bilayer with OPLS3e force field, 1000 mM CaCl2 part 2. 2022, DOI: 10.5281/zenodo.6352681.

63. Han K, Venable RM, Bryant A, Legacy CJ, Shen R, Li H, et al. Graph–Theoretic Analysis of Monomethyl Phosphate Clustering in Ionic Solutions. J Phys Chem B. 2018 -02-01;122(4):1484-94.

64. Lindström M. MD simulation of POPC bilayer with CHARMM36 force field, 100 mM NaCl. 2022, DOI: 10.5281/zenodo.6342104.

65. Lindström M. MD simulation of POPC bilayer with CHARMM36 force field, 200 mM NaCl. 2022, DOI: 10.5281/zenodo.6342175.

66. Lindström M. MD simulation of POPC bilayer with CHARMM36 force field, 500 mM NaCl. 2022, DOI: 10.5281/zenodo.6342522.

67. Lindström M. MD simulation of POPC bilayer with CHARMM36 force field, 1000 mM NaCl. 2022, DOI: 10.5281/zenodo.6342652.

68. Lindström M. MD simulation of POPC bilayer with CHARMM36 force field, 50 mM CaCl2. 2022, DOI: 10.5281/zenodo.6341899.

69. Lindström M. MD simulation of POPC bilayer with CHARMM36 force field, 100 mM CaCl2. 2022, DOI: 10.5281/zenodo.6341420.

70. Lindström M. MD simulation of POPC bilayer with CHARMM36 force field, 200 mM CaCl2. 2022, DOI: 10.5281/zenodo.6337813.

71. Lindström M. MD simulation of POPC bilayer with CHARMM36 force field, 500 mM CaCl2. 2022, DOI: 10.5281/zenodo.6339898.

72. Lindström M. MD simulation of POPC bilayer with CHARMM36 force field, 1000 mM CaCl2. 2022, DOI: 10.5281/zenodo.6337490.

73. Berendsen H, Postma JPM, van Gunsteren W, Hermans J. Interaction Models for Water in Relation to Protein Hydration. In: Intermol Forces. ; 1981. p. 331-42.

74. Jorgensen WL, Chandrasekhar J, Madura JD, Impey RW, Klein ML. Comparison of simple potential functions for simulating liquid water. J Chem Phys. 1983 July 15,;79(2):926-35.

75. Martyna GJ, Tobias DJ, Klein ML. Constant pressure molecular dynamics algorithms. J Chem Phys. 1994 September 1,;101(5):4177-89.

76. Martyna GJ, Klein ML, Tuckerman M. Nosé–Hoover chains: The canonical ensemble via continuous dynamics. J Chem Phys. 1992 August 15,;97(4):2635-43.

77. Jo S, Kim T, Iyer VG, Im W. CHARMM-GUI: A web-based graphical user interface for CHARMM. Journal of Computational Chemistry. 2008;29(11):1859-65.

78. Durell SR, Brooks BR, Ben-Naim A. Solvent-Induced Forces between Two Hydrophilic Groups. J Phys Chem. 1994 -02-01;98(8):2198-202.

79. Neria E, Fischer S, Karplus M. Simulation of activation free energies in molecular systems. J Chem Phys. 1996 August 1,;105(5):1902-21.

80. Nosé S. A molecular dynamics method for simulations in the canonical ensemble. Molecular Physics. 1984 June 10,;52(2):255-68.

81. Hoover WG. Canonical dynamics: Equilibrium phase-space distributions. Phys Rev A. 1985;31(3):1695-7.

82. Parrinello M, Rahman A. Polymorphic transitions in single crystals: A new molecular dynamics method. Journal of Applied Physics. 1981 December 1,;52(12):7182-90.

83. Ollila OHS and et al. Match github repository. github.com/NMRlipids/MATCH

84. Michaud-Agrawal N, Denning EJ, Woolf TB, Beckstein O. MDAnalysis: a toolkit for the analysis of molecular dynamics simulations. J Comput Chem. 2011 Jul 30,;32(10):2319-27.

85. Gowers RJ, Linke M, Barnoud J, Reddy TJE, Melo MN, Seyler SL., Domanski J, Dotson DL, Buchoux S, Kenney IM, Beckstein O. MDAnalysis: A Python package for the rapid analysis of molecular dynamics simulations. In S. Benthall and S. Rostrup, editors, Proceedings of the 15th Python in Science Conference, pages 98-105, Austin, TX, 2016. SciPy, doi:10.25080/majora-629e541a-00e.

86. Humphrey W, Dalke A, Schulten K. VMD} -- {V}isual {M}olecular {D}ynamics. Journal of Molecular Graphics. 1996;14:33-8.

87. Shirts MR, Klein C, Swails JM, Yin J, Gilson MK, Mobley DL. Case DA, Zhong ED. Lessons learned from comparing molecular dynamics engines on the SAMPL5 dataset. Journal of computer-aided molecular design. 2016:1-15.

88. Seelig J, Waespe-Sarcevic N. Molecular order in cis and trans unsaturated phospholipid bilayers. Biochemistry. 1978 -08-08;17(16):3310-5.

89. Gally HU, Pluschke G, Overath P, Seelig J. Structure of Escherichia coli membranes. Glycerol auxotrophs as a tool for the analysis of the phospholipid head-group region by deuterium magentic resonance. Biochemistry. 1981 -03-31;20(7):1826-31.

90. Engel AK, Cowburn D. The origin of multiple quadrupole couplings in the deuterium NMR spectra of the 2 chain of 1,2 dipalmitoyl-sn-glycero-3-phosphorylcholine. FEBS Lett. 1981 -04-20;126(2):169-71.

91. Bechinger B, Seelig J. Conformational changes of the phosphatidylcholine headgroup due to membrane dehydration. A 2H-NMR study. Chemistry and Physics of Lipids. 1991 May 1,;58(1):1-5.

92. Seelig J, Macdonald PM, Scherer PG. Phospholipid head groups as sensors of electric charge in membranes. Biochemistry. 1987 -12-01;26(24):7535-41.

93. Akutsu H, Seelig J. Interaction of metal ions with phosphatidylcholine bilayer membranes. Biochemistry. 1981 -12-01;20(26):7366-73.

94. Altenbach C, Seelig J. Calcium binding to phosphatidylcholine bilayers as studied by deuterium magnetic resonance. Evidence for the formation of a calcium complex with two phospholipid molecules. Biochemistry. 1984 -08-01;23(17):3913-20.

95. Venable RM, Luo Y, Gawrisch K, Roux B, Pastor RW. Simulations of anionic lipid membranes: development of interaction-specific ion parameters and validation using NMR data. J Phys Chem B. 2013 Sep 05,;117(35):10183-92.

96. Arkhipov A, Shan Y, Das R, Endres NF, Eastwood MP, Wemmer DE, et al. Architecture and membrane interactions of the EGF receptor. Cell. 2013 -01-31;152(3):557-69.

97. Kaszuba K, Grzybek M, Orłowski A, Danne R, Róg T, Simons K, et al. N-Glycosylation as determinant of epidermal growth factor receptor conformation in membranes. Proc Natl Acad Sci U S A. 2015 -04-07;112(14):4334-9.

98. Lu C, Wu C, Ghoreishi D, Chen W, Wang L, Damm W, et al. OPLS4: Improving Force Field Accuracy on Challenging Regimes of Chemical Space. Journal of chemical theory and computation. 2021 07/13/;17(7).

Supporting information:

Structure of POPC lipid bilayers in OPLS3e force field

Milla Lindström[1], Antti Poso[1], Piia Bartos[1]‡, Markus S. Miettinen[2*]‡*

Content

1. Impact of TIP3P water model in OPLS3e
2. Order parameters in response to additional salt
3. Equilibration times of the ion binding and impact on order parameters
4. Scaling the ion charge in OPLS3e
5. Small bug in CHARMM36 parameters
6. Effect of temperature change in CHARMM36

1. Impact of TIP3P water model in OPLS3e

To clarify if water model has an impact on cation binding affinity of membranes in OPLS3e, we performed simulations using TIP3P water model instead of SPC with 1000 mM concentration of NaCl or $CaCl_2$ and without ions. Without ions (Fig. 1) and at 1000 mM concentrations (Fig. 2) TIP3P produced similar order parameters as SPC, suggesting that there is no major difference between SPC and TIP3P water models in OPLS3e with or without ions.

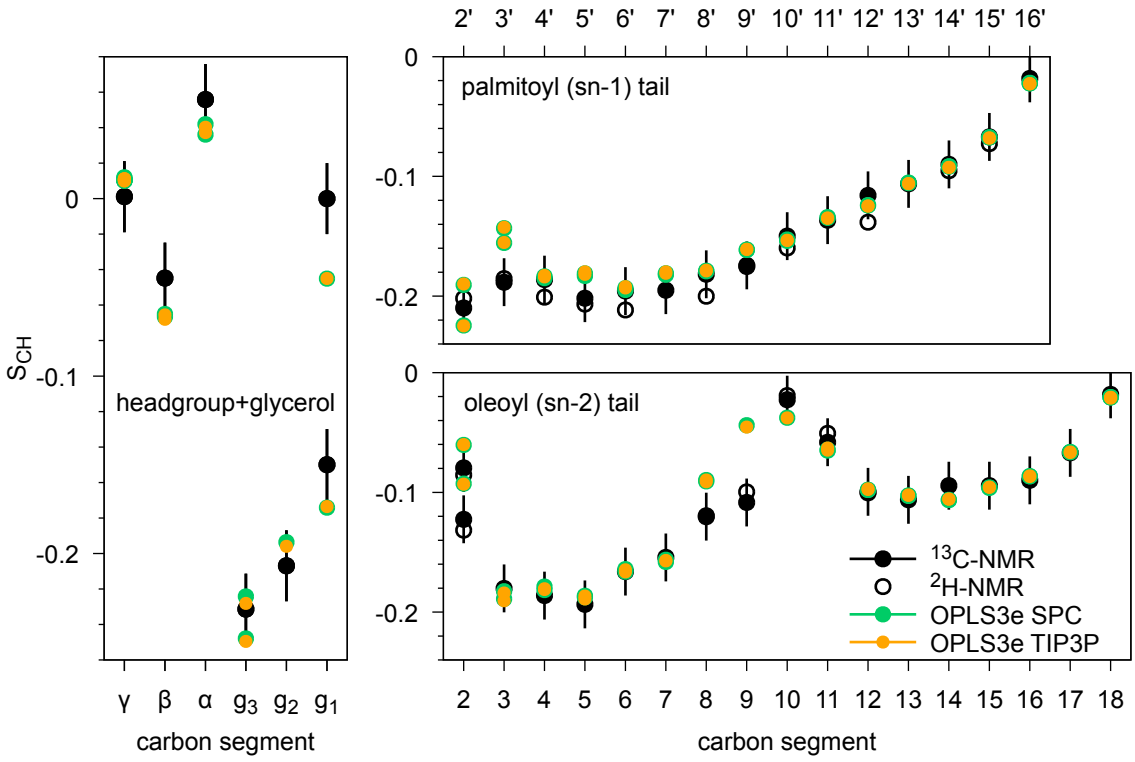

Figure 1. Order parameters at full hydration for headgroup, backbone, and acyl chains in OPLS3e with SPC and TIP3P water models. Experimental values for the POPC (^{1}H- ^{13}C NMR) at 300 K are from Ref. 1 and ^{2}H-NMR are from Ref. 2. Simulations are also for POPC.

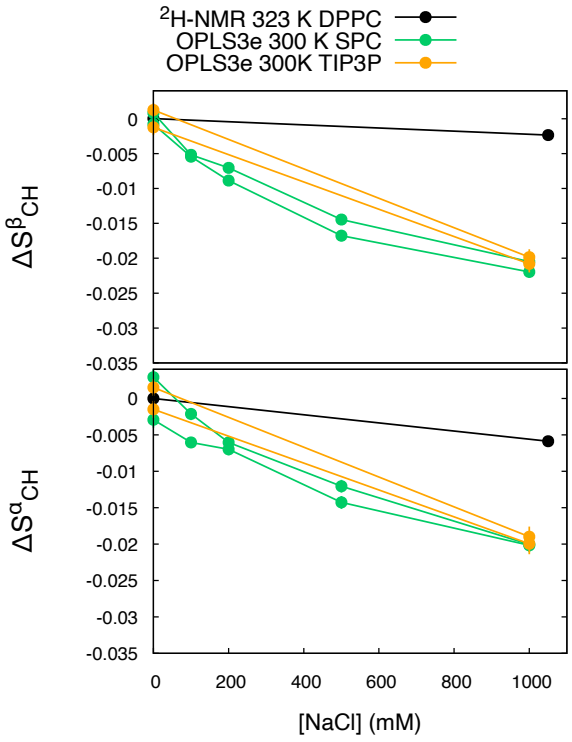

Figure 2. Change of order parameters in headgroup α and β segments in response to rising concentration of NaCl. Experimental values for DPPC (^{2}H NMR) at 323 K are from Ref. 3. Simulations POPC. The average C–H bond order parameters of R and S hydrogens were used to calculate the difference between the baseline and different salt concentrations.

2. Order parameters in response to additional salt

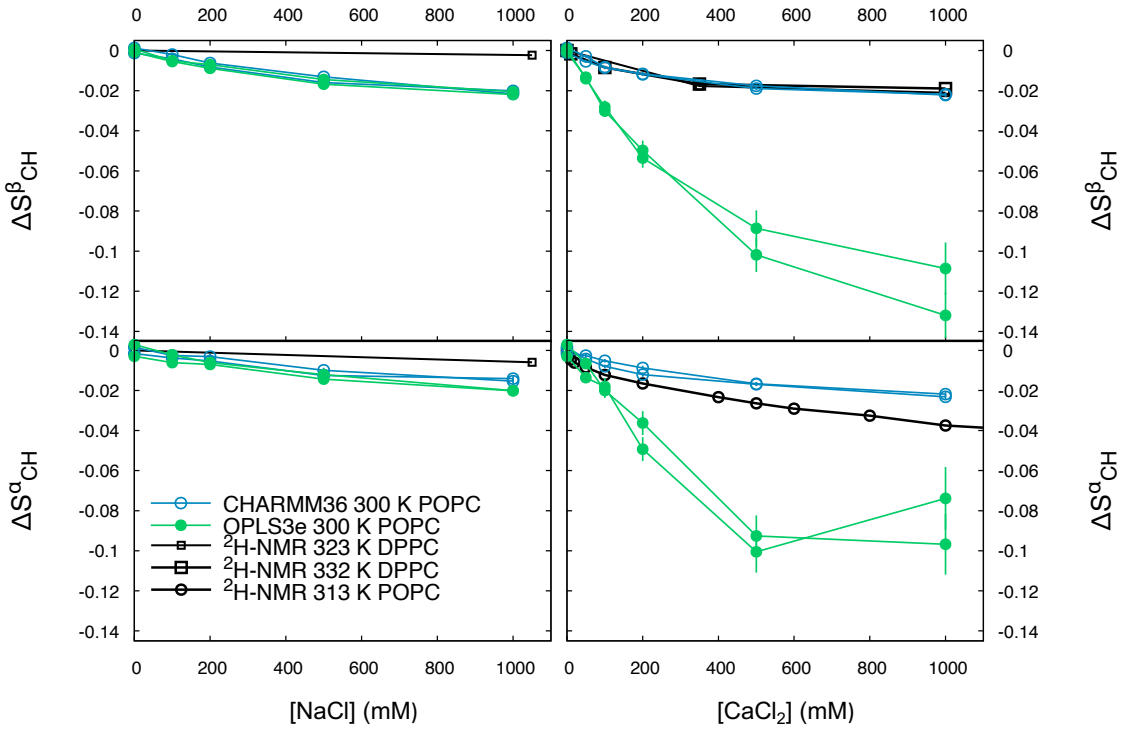

Figure 3. Change of order parameters in the headgroup α and β segments in response to rising concentration of NaCl or $CaCl_2$ as a full figure. Experimental values for DPPC (^{2}H NMR) at 323 K and 332 K are from Ref. 3 and for POPC (^{2}H NMR) at 313 K are from Ref. 4. The average C–H bond order parameters of R and S hydrogens were used to calculate the difference between the baseline and different salt concentrations.

3. Equilibration times of the ion binding and impact on order parameters

Our simulations show that quite long equilibration time is needed for ion binding to the membrane in OPLS3e (both Ca^{2+} and Cl^-) as the number of ions keeps rising in the vicinity of membrane (Fig. 4). 200 mM and higher concentrations seem to require (almost) the whole 1 μs simulation to reach final equilibrium. Catte et al. reported similar results over 1000 ns equilibration time for $CaCl_2$ in original CHARMM36 (no NBfix) (5). In our simulations, CHARMM36 with NBfix parameters does not induce ions to bind to membrane with high

affinity and equilibration is consequently faster (Fig. 5). S^{α}_{CH} and S^{β}_{CH} also show decline as a function of simulation time in OPLS3e as the number of ions in vicinity of the membrane keeps rising, see Fig. 4 but not in CHARMM36 (Fig. 5).

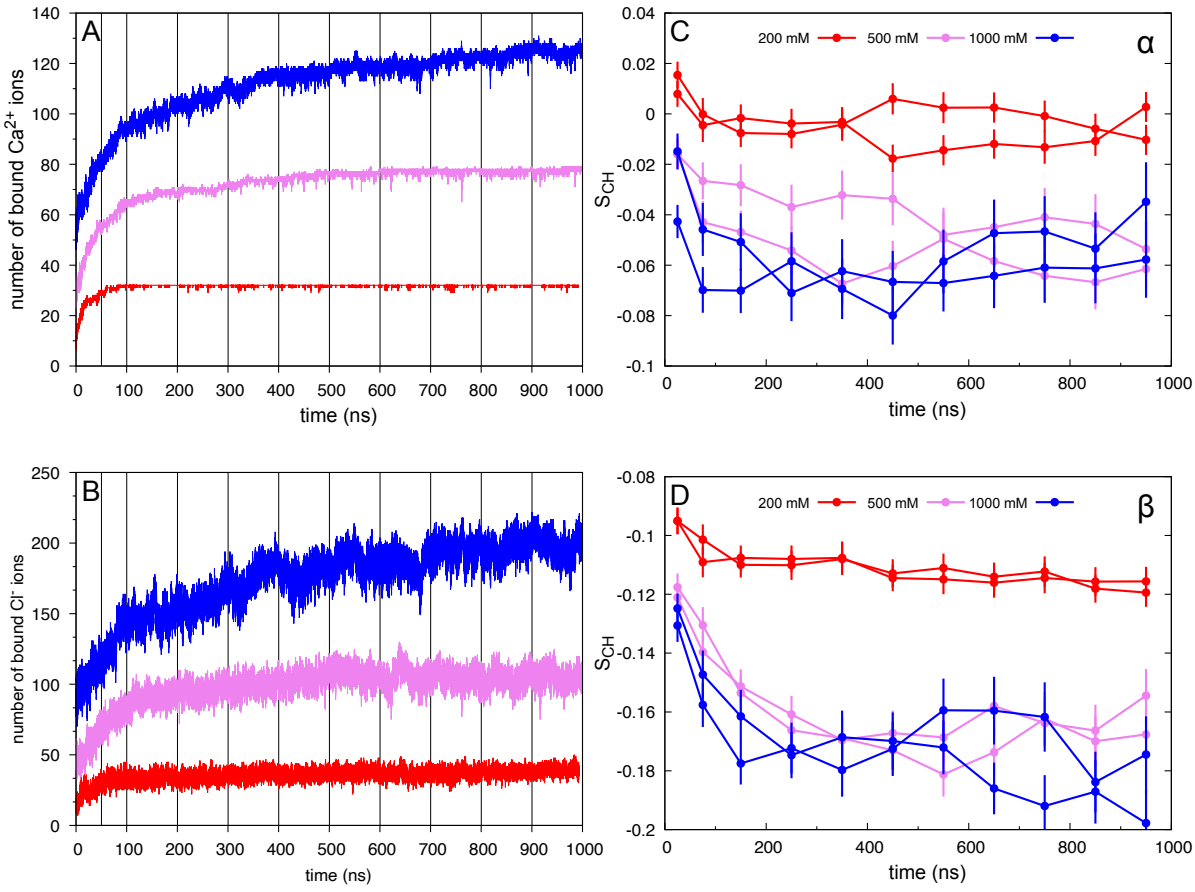

Figure 4. Number of (A) Ca^{2+} (B) Cl^{-} ions within 2.5 nm from bilayer center. (C) S^{α}_{CH} and (D) S^{β}_{CH} as a function of simulation time in OPLS3e with additional $CaCl_2$ 200, 500, and 1000 mM concentrations. Order parameters in C and D panels calculated for trajectory pieces show with vertical lines in A and B panels.

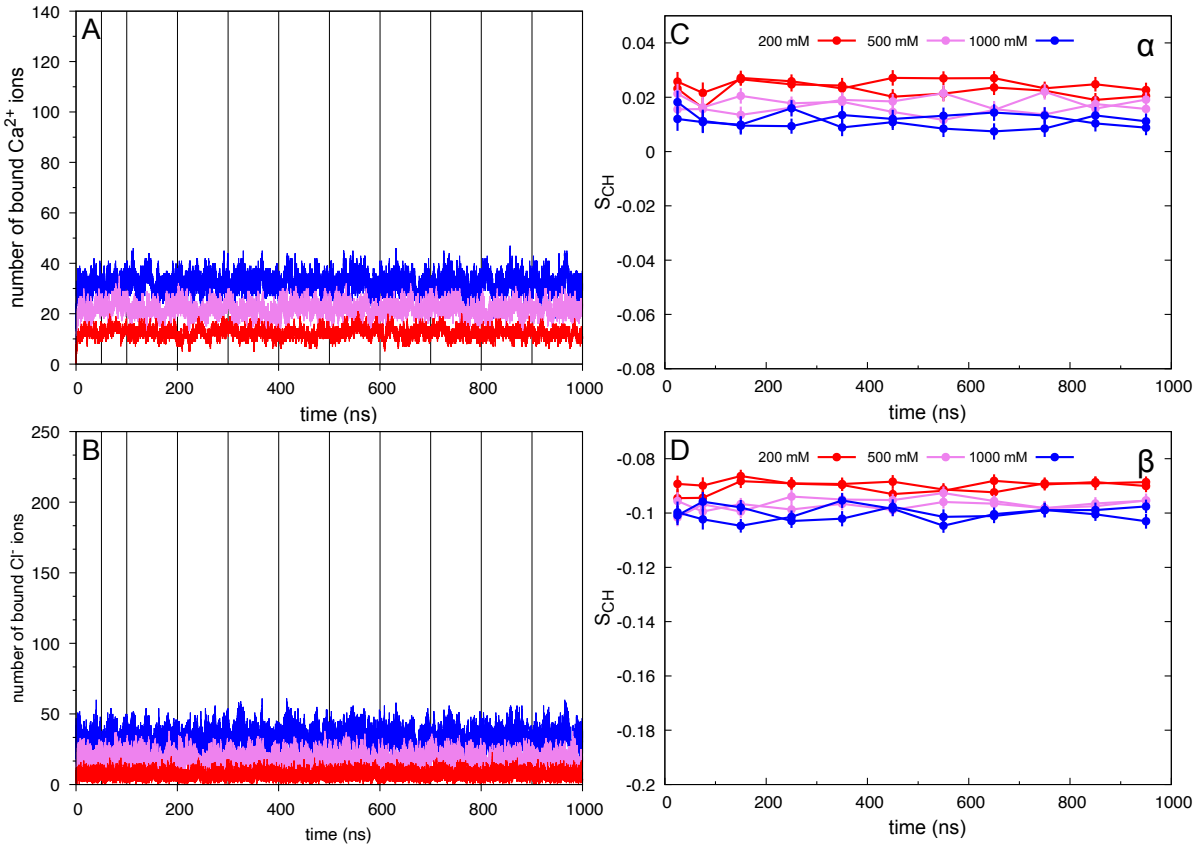

Figure 5. Number of (A) Ca^{2+} (B) Cl^- ions within 2.5 nm from bilayer center. (C) S^{α}_{CH} and (D) S^{β}_{CH} as a function of simulation time in CHRMM36 with additional $CaCl_2$ 200, 500, and 1000 mM concentrations. Order parameters in C and D panels calculated for trajectory pieces show with vertical lines in A and B panels.

4. Scaling the ion charge in OPLS3e

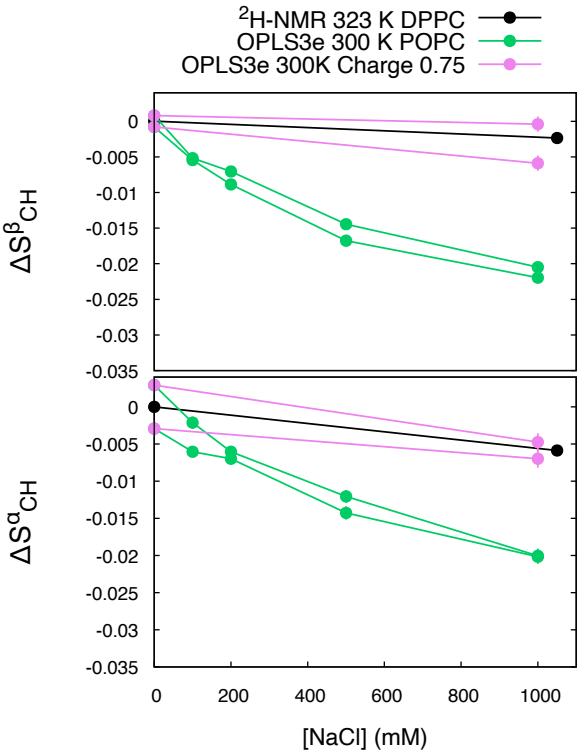

Figure 6. Change of order parameters in the POPC headgroup α and β segments in response to additional NaCl in OPLS3e force field with scaled and unscaled ions. Scaling was done with the factor of 0.75 for the charge of both Na^+ and Cl^- ions. Experimental values for DPPC (^{2}H NMR) at 323 K are from Ref. 3. The average C–H bond order parameters of R and S hydrogens were used to calculate the difference between the baseline and different salt concentrations.

Over binding of ions to membranes is a problem in most of the current force fields and based on our studies this is the case also with OPLS3e force field. One reason behind the over binding might be too high charge of the ions. In previous studies, it has been proposed that scaling the ion charge might help to overcome mistakes resulting from the lacking electronic polarization (6, 7). In electronic continuum correlation (ECC) theory, based on quantum mechanical calculations, scaling factor of ions is 0.75. This scaling of ion charges has been able to improve monovalent ion binding in some force fields, but has not been sufficient for the divalent $CaCl_2$. To further investigate behavior of ions in OPLS3e we scaled the charge of monovalent NaCl and divalent $CaCl_2$ by factor 0.75, as in ECC theory, and performed simulations using 1000

mM concentrations with scaled charges. Scaling enhanced order parameters for the alpha and beta carbons in the presence of additional 1000 mM NaCl (Fig. 6) but was not sufficient for $CaCl_2$ (Fig. 7). However, with scaled charged of $CaCl_2$, ion binding to membrane equilibrates much faster than with unscaled charges (Fig. 8)

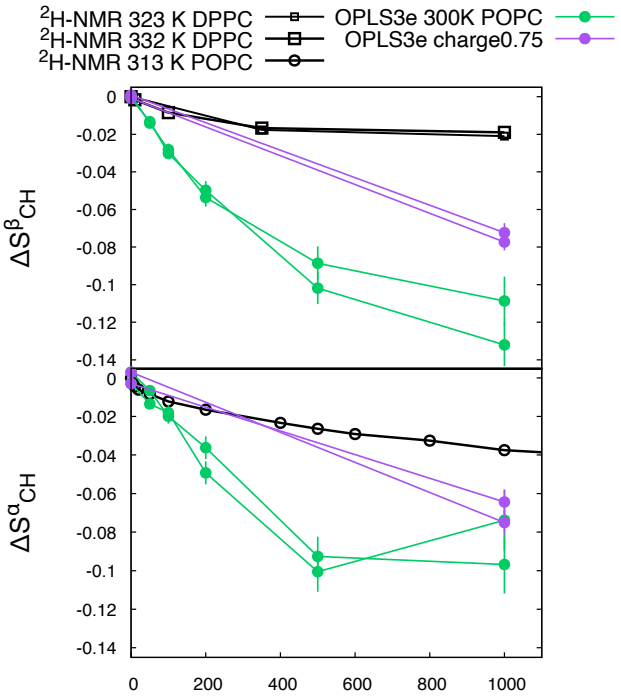

Figure 7. Change of order parameters in the POPC headgroup α and β segments in response to additional $CaCl_2$ in OPLS3e force field with scaled and unscaled ions. Scaling was done with the factor of 0.75 for the charge of both Ca^{2+} (charge 1.5) and Cl^- ions. Experimental values for DPPC (^{2}H NMR) at 323 K and 332 K are from Ref. 3 and for POPC (^{2}H NMR) at 313 K are from Ref. 4. The average C–H bond order parameters of R and S hydrogens were used to calculate the difference between the baseline and different salt concentrations. Last 100 ns of 1000 ns trajectory was used for analysis for unscaled ions, and last 400 ns of 500 ns trajectory for scaled ions.

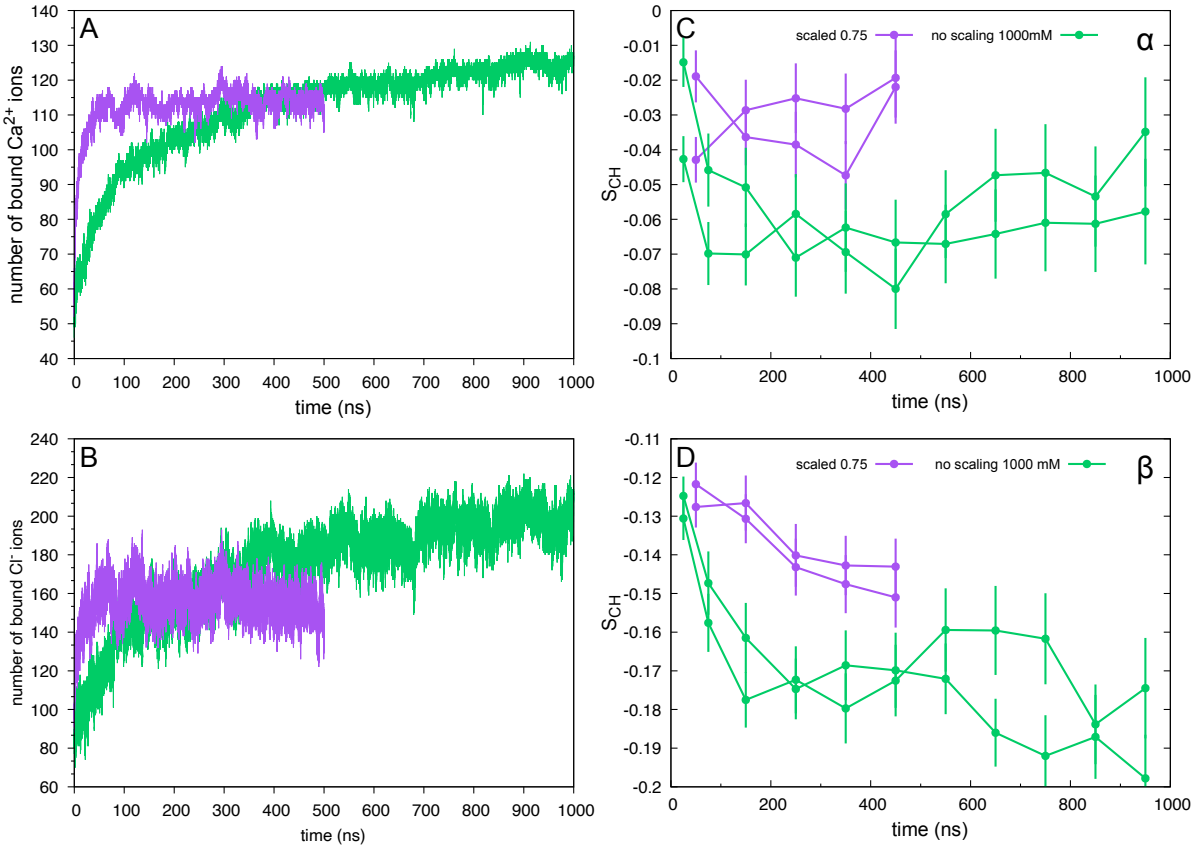

Figure 8. Number of (A) Ca^{2+} (B) Cl^- ions within 2.5 nm from bilayer center. (C) S^{α}_{CH} and (D) S^{β}_{CH} as a function of simulation time in OPLS3e with additional 1000 mM scaled and unscaled $CaCl_2$.

The over binding of Ca^{2+} cannot be easily fixed by scaling the charge of the ions (or by adding non-bonded fix parameters). To this end, Melcr et al. extended the ECC theory to include also partial charges of the polar region of POPC phospholipids to build the ECC-POPC model based on the Lipid14 force field (they also did this for CHARMM36 with same scaling) (7). The resulting ECC-POPC model produces experimental order parameter responses to NaCl and even for divalent $CaCl_2$ unlike any other current force field, and can thus be considered as one of the most realistic models to describe POPC lipid membrane in the presence of ions so far.

5. Small bug in CHARMM36 parameters

We noticed a small bug in the CHARMM36 force field parameters obtained at the time of the research (summer 2020) from CHARMM-GUI. Parameters were missing following dihedral line:

```
316a317
> CTL2  CEL1  CEL1  HEL1   9 1.800000e+02 2.510400e+01    2
```

By the end of 2020, the parameters in CHARMM-GUI were fixed. We compared the order parameters from simulations performed with parameters without (bug) and with the dihedral (bugfix) and discovered that there was no difference in order parameters between those parameter sets (Fig 9). However, we have used CHARMM36 bugfix parameters in all the simulations presented in this paper.

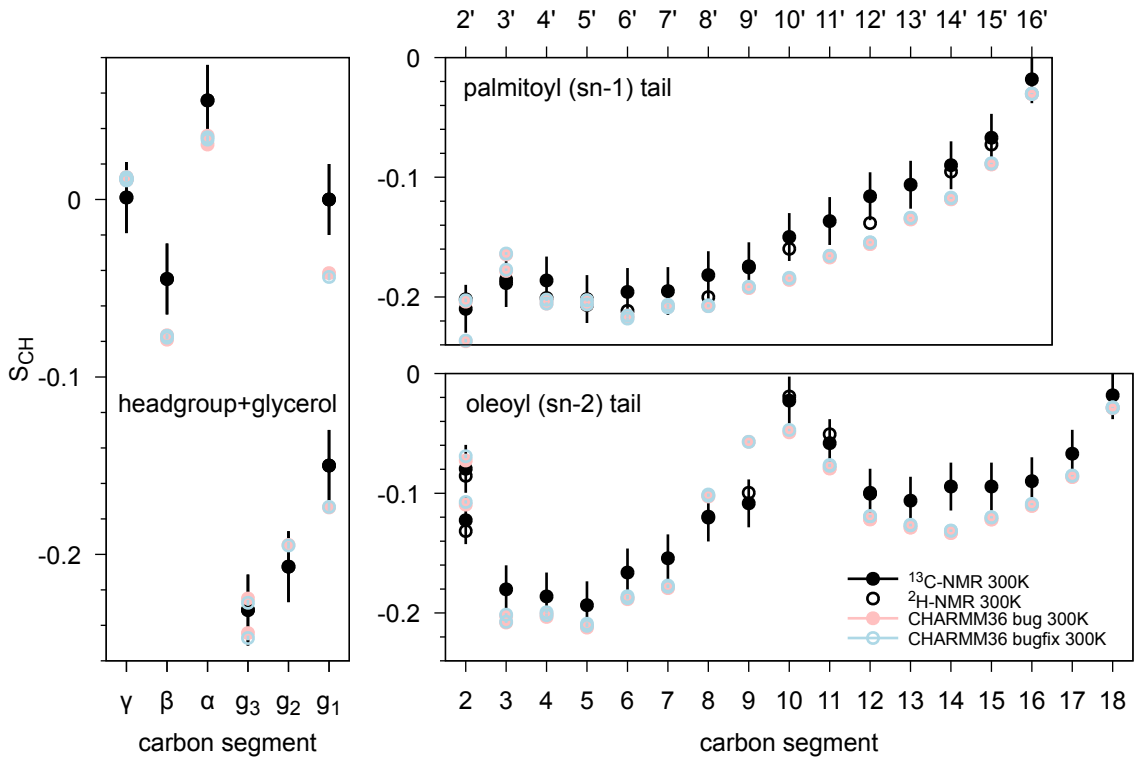

Figure 9. Order parameters for POPC in CHARMM36 with a bug compared to parameters with bugfix for headgroup, backbone, and acyl chains. Experimental values for the POPC (^{1}H-^{13}C NMR) at 300 K are from Ref. 1 and ^{2}H-NMR are from Ref. 2.

6. Effect of temperature change in CHARMM36

In addition to 300 K, we simulated some CHARMM36 systems also using 314 K temperature. We can see that order parameters at full hydration are in general slightly higher at 314 K than 300 K (Fig. 10). Lowering hydration induces similar responses in both temperatures, but 314 K does not induce forking in 5 w/l hydration in contrast to 300 K (Fig. 11). Slight changes in order parameters might be linked to temperature-induced changes in area per lipid. At 314 K the area per lipid is larger, which allows lipids to move more than at 300 K (Fig. 12).

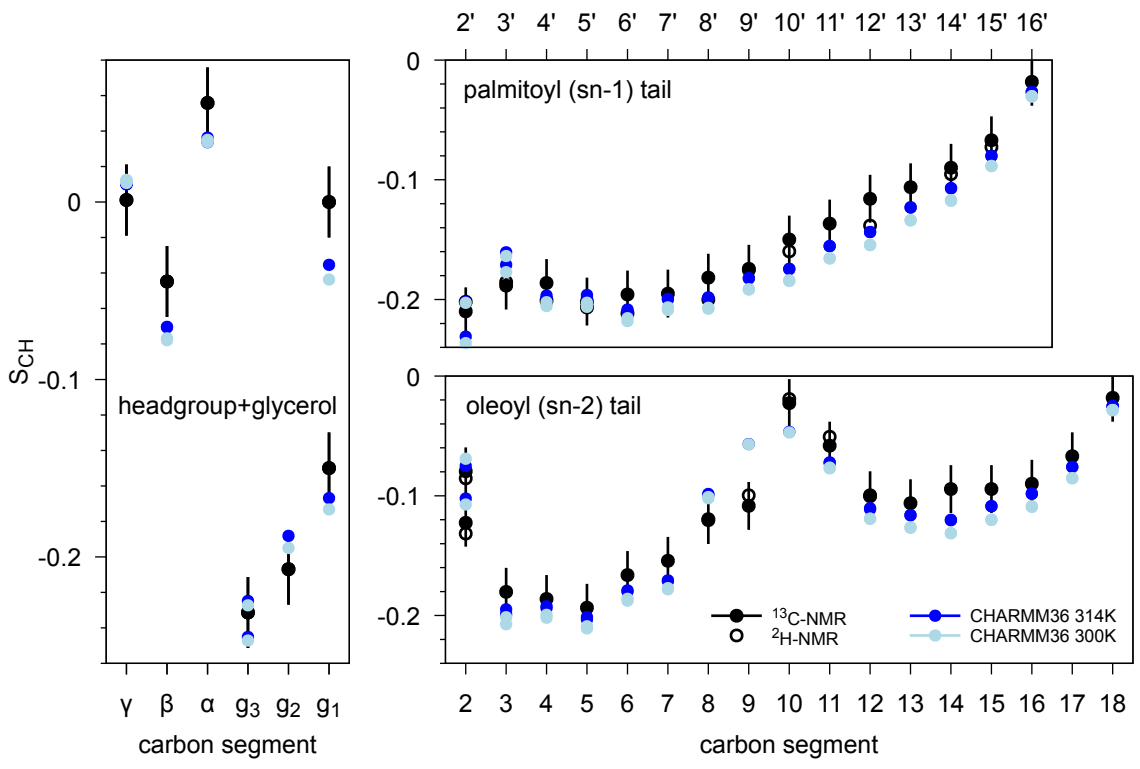

Figure 10. Order parameters at full hydration (33 waters/lipid) for POPC headgroup and backbone acyl chains in simulations and experiments. Experimental values for the POPC (^{1}H-^{13}C NMR) at 300 K are from Ref. (1) and ^{2}H-NMR are from Ref. (2).

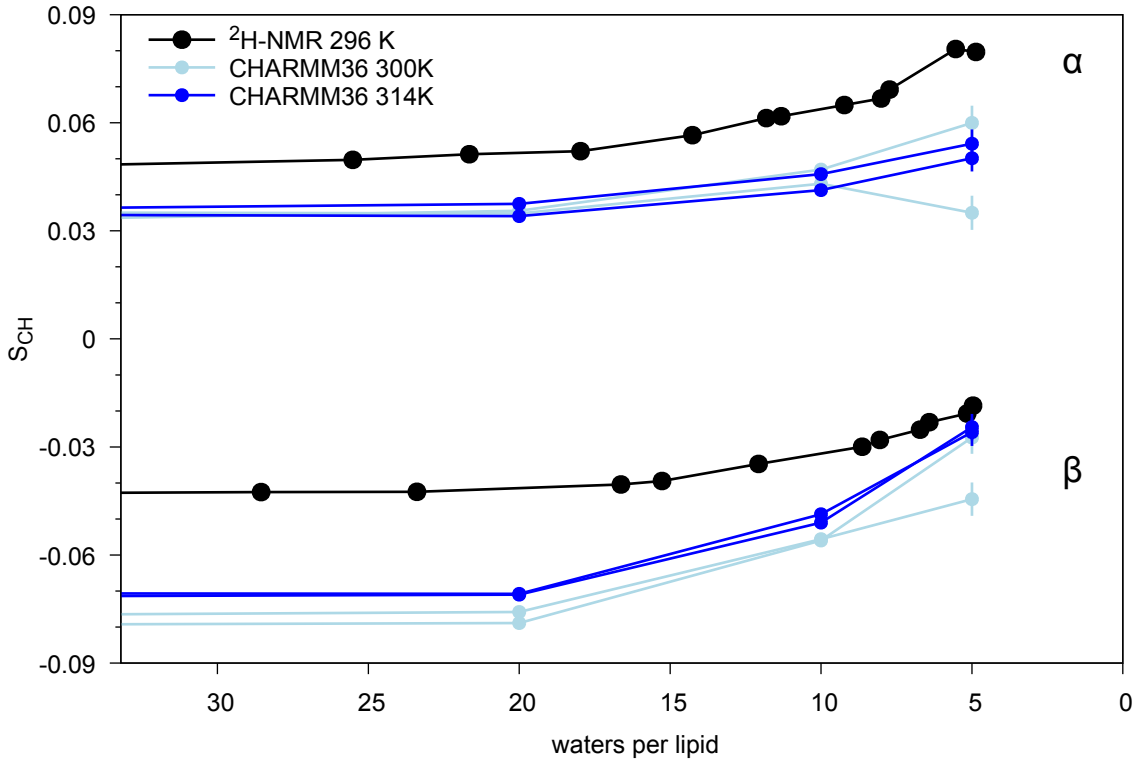

Figure 11. Order parameters in response to decreasing hydration level for the headgroup α and β carbons. Experimental values for POPC (^{2}H NMR) at 296 K are from Ref. (8).

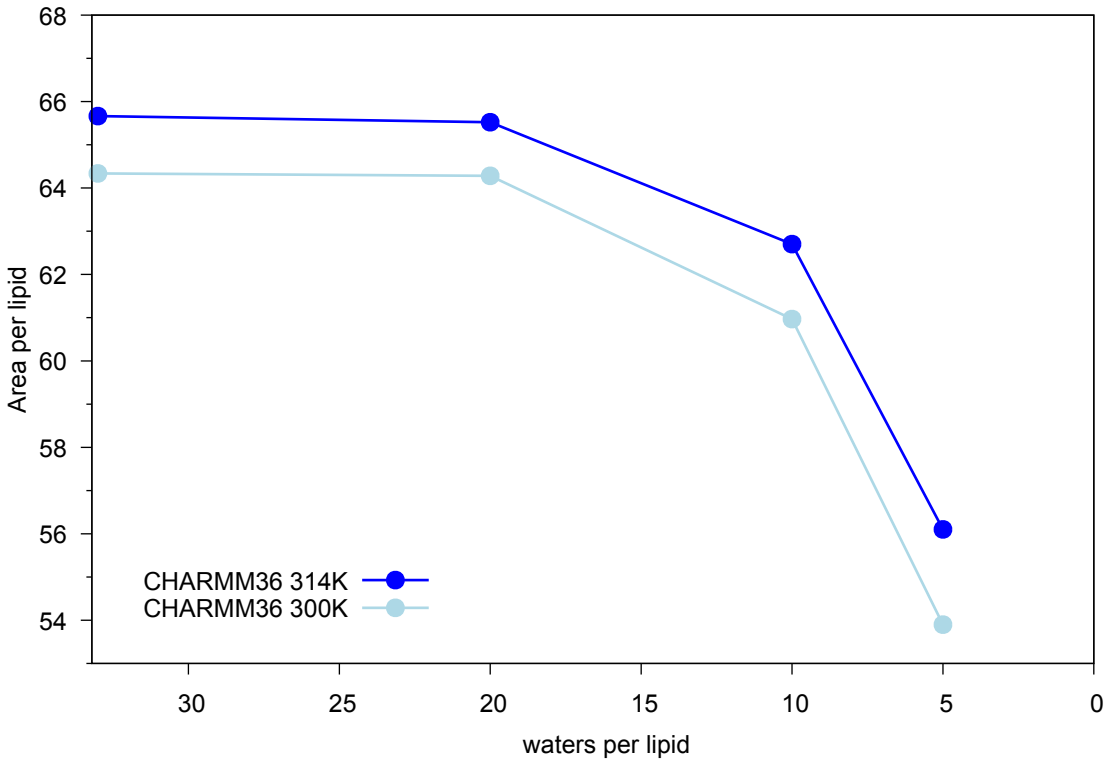

Figure 12. Area per lipid in response to lowering hydration level in CHARMM36 with 300 K and 314 K temperatures.

References

1. Ferreira TM, Coreta-Gomes F, Ollila OHS, Moreno MJ, Vaz WLC, Topgaard D. Cholesterol and POPC segmental order parameters in lipid membranes: solid state 1H–13C NMR and MD simulation studies. Phys Chem Chem Phys. 2013 -01-16;15(6):1976-89.

2. Seelig J, Waespe-Sarcevic N. Molecular order in cis and trans unsaturated phospholipid bilayers. Biochemistry. 1978 -08-08;17(16):3310-5.

3. Akutsu H, Seelig J. Interaction of metal ions with phosphatidylcholine bilayer membranes. Biochemistry. 1981 -12-01;20(26):7366-73.

4. Altenbach C, Seelig J. Calcium binding to phosphatidylcholine bilayers as studied by deuterium magnetic resonance. Evidence for the formation of a calcium complex with two phospholipid molecules. Biochemistry. 1984 -08-01;23(17):3913-20.

5. Catte A, Girych M, Javanainen M, Loison C, Melcr J, Miettinen MS, et al. Molecular electrometer and binding of cations to phospholipid bilayers. Phys Chem Chem Phys. 2016 Nov 30,;18(47):32560-9.

6. Kohagen M, Mason PE, Jungwirth P. Accounting for Electronic Polarization Effects in Aqueous Sodium Chloride via Molecular Dynamics Aided by Neutron Scattering. J Phys Chem B. 2016 -03-03;120(8):1454-60.

7. Melcr J, Martinez-Seara H, Nencini R, Kolafa J, Jungwirth P, Ollila OHS. Accurate Binding of Sodium and Calcium to a POPC Bilayer by Effective Inclusion of Electronic Polarization. J Phys Chem B. 2018 April 26,;122(16):4546-57.

8. Bechinger B, Seelig J. Conformational changes of the phosphatidylcholine headgroup due to membrane dehydration. A 2H-NMR study. Chemistry and Physics of Lipids. 1991 May 1,;58(1):1-5.